Utilizing anaerobic substrate distribution for growth of aerobic granular sludge in continuous-flow reactors

Haaksman, Viktor A.; van Dijk, Edward J.H.; Al-Zuhairy, Salah; Mulders, Michel; Loosdrecht, Mark C.M.van; Pronk, Mario

DOI
10.1016/j.watres.2024.121531

Publication date
2024

Document Version
Final published version

Published in
Water Research

Water Research 257 (2024) 121531

Contents lists available at ScienceDirect

Water Research

journal homepage: www.elsevier.com/locate/watres

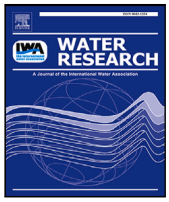

Utilizing anaerobic substrate distribution for growth of aerobic granular sludge in continuous-flow reactors

Viktor A. Haaksman [b,1,*], Edward J.H. van Dijk [c,1], Salah Al-Zuhairy [b], Michel Mulders [b], Mark C.M. van Loosdrecht [a], Mario Pronk [a,c,*]

[a] Department of Biotechnology, Delft University of Technology, Van der Maasweg 9, Delft, 2629 HZ, The Netherlands
[b] Delfluent Services, Peuldreef 4, Den Hoorn, 2635 BX, The Netherlands
[c] Royal HaskoningDHV, Laan 1914 35, Amersfoort, 3800 AL, The Netherlands

ARTICLE INFO

Keywords:
Municipal wastewater
Continuous flow reactor
Aerobic granular sludge
Selective feeding
Selective wasting
Anaerobic substrate distribution

ABSTRACT

The development of continuous flow reactors (CFRs) employing aerobic granular sludge (AGS) for the retrofit of existing wastewater treatment plants (WWTPs) using a continuous-flow activated sludge (CFAS) system has garnered increasing interest. This follows the worldwide adoption of AGS technology in sequencing batch reactors (SBRs). The better settleability of AGS compared to AS allows for process intensification of existing wastewater treatment plants without the difficult conversion of often relatively shallow CFRs to deeper AGS-SBRs.

To retrofit existing CFAS systems with AGS, achieving both increased hydraulic capacity and enhanced biological nutrient removal necessitates the formation of granular sludge based on the same selective pressures applied in AGS-SBRs. Previous efforts have focussed mainly on the selective wasting of flocculent sludge and retaining granular sludge to drive aerobic granulation.

In this study a pilot-scale CFR was developed to best mimic the implementation of the granulation mechanisms of full-scale AGS-SBRs. The pilot-scale reactor was fed with pre-settled municipal wastewater. We established metrics to assess the degree to which the proposed mechanisms were implemented in the pilot-scale CFR and compared them to data from full-scale AGS-SBRs, specifically with respect to the anaerobic distribution of granule forming substrates (GFS). The selective pressures for granular sludge formation were implemented through inclusion of anaerobic upflow selectors with a water depth of 2.5 meters, which yielded a sludge with properties similar to AGS from full-scale SBRs. In comparison to the CFAS system at Harnaschpolder WWTP treating the same pre-settled wastewater, a more than twofold increase in volumetric removal capacity for both phosphorus and nitrogen was achieved. The use of a completely mixed anaerobic selector, as opposed to an anaerobic upflow selector, caused a shift in EBPR activity from the largest towards the smallest size class, while nitrification was majorly unaffected. Anaerobic selective feeding via bottom-feeding is, therefore, favorable for the long-term stability of AGS, especially for less acidified wastewater. The research underlines the potential of AGS for enhancing the hydraulic and biological treatment capacity of existing CFAS systems.

1. Introduction

The development of continuous flow reactors (CFRs) employing aerobic granular sludge (AGS) for the retrofit of existing wastewater treatment plants with a continuous-flow activated sludge (CFAS) system has received increasing interest following the world-wide adoption of the AGS technology in sequencing batch reactors (SBRs), commercialized as Nereda® (Giesen et al., 2013; Pronk et al., 2015). The better settleability of AGS compared to AS allows for process intensification of existing treatment facilities without the difficult conversion of often relatively shallow CFRs to deeper SBRs (Winkler and van Loosdrecht, 2022).

To fulfill the promise of AGS in CFRs, the process conditions necessary for sufficient granular growth must be adapted from full-scale AGS-SBRs. CFAS systems designed for enhanced biological phosphorus removal (EBPR), which have been developed to yield well settling flocculent sludge and prevent filamentous bulking (Martins et al., 2004b), share process characteristics with AGS-SBRs with respect to the anaerobic stage (Daigger et al., 2018). A plug-flow anaerobic selector with

* Corresponding authors.
E-mail addresses: v.a.haaksman@tudelft.nl (V.A. Haaksman), m.pronk@tudelft.nl (M. Pronk).
[1] Both authors contributed equally to this manuscript.

https://doi.org/10.1016/j.watres.2024.121531
Received 17 November 2023; Received in revised form 24 March 2024; Accepted 26 March 2024
Available online 28 March 2024

a high initial readily biodegradable chemical oxygen demand (rbCOD) loading rate provides penetration depth into the flocs and ensures complete conversion of the rbCOD to storage polymers, prior to the aeration stage, to prevent transport-limited substrate uptake (Martins et al., 2004a). A strong rbCOD concentration gradient in the expanded bed during bottom-feeding is the equivalent in AGS-SBRs (van Dijk et al., 2018). Considering this similarity, spontaneous aerobic granulation events in CFAS systems have been reported (Redmond et al., 2019). In all cases an SVI_{30} similar to AGS from full-scale SBRs was found (Pronk et al., 2015; van Dijk et al., 2020), although the mean granule sizes were smaller (i.e. <1 mm) (Wei et al., 2020). No significant quantitative correlations between operational parameters and the fraction of granular sludge (i.e. >200 μm) could be determined. The degree of granulation was positively correlated with the increased enrichment for phosphate accumulating organisms (PAO) and glycogen accumulating organisms (GAO) in the granular sludge relative to flocculent sludge fraction in the study by Wei et al. (2020). This underlines once again the importance of the selection for slow-growing heterotrophic bacteria as a driver of aerobic granulation (De Kreuk and Van Loosdrecht, 2004).

Full-scale endeavors to enhance settling characteristics has mainly focused on the selective retention of better settling sludge (Daigger et al., 2023). An external selector to keep better settling fraction in the sludge can be readily implemented on existing WWTPs (Ford et al., 2016). Selective wasting based on differences in density or particle size using hydrocyclones have yielded better settling (densified) AS with diluted sludge volume indices ($dSVI_{30}$) (Roche et al., 2022; Ford et al., 2016; Gemza et al., 2022; Avila et al., 2021). This is akin to the undiluted SVI_{30} of AGS from full-scale SBRs (Pronk et al., 2015), although the degree of granulation varied and the mean granule sizes were <1 mm (Daigger et al., 2023). Apart from stabilization of the sludge settleability, an increase in hydraulic or biological treatment capacity of an existing CFAS system has not yet been reported using external selectors alone.

In contrast, the hallmark of AGS in SBRs is the combination of increased settleability and higher volumetric nutrient removal rates. This combination allows for both higher surface loading rates of final clarifiers and greater biological treatment capacity. These factors are crucial for a retrofit concept for CFAS systems based on AGS. Increased nutrient removal rates are achieved through higher MLSS concentrations and strong nutrient concentrations during the aerated phase of an SBR. These conditions result in sufficient penetration depth to effectively utilize the full potential of granular biomass (Pronk et al., 2015). Full-scale AGS-SBRs achieve higher MLSS concentrations of granular sludge, while controlling the concentration of flocculent sludge, which limits the overall sludge volume (van Dijk et al., 2020). The diluted SVI_{30} of densified AS can be similar to the undiluted SVI_{30} of full-scale AGS (Roche et al., 2022). However, the relatively higher coherence of densified AS compared to AGS (Roche et al., 2022) means that the settling occurs more in the compression regime at higher MLSS concentrations, and this decreases overall settleability. This also limits sludge loading to a final clarifier, and thereby limits the potential for increase of the total sludge concentration in the aeration stage.

To upgrade CFAS systems designed with biological nutrient removal (BNR) with additional capacity through AGS, the selective pressures from full-scale AGS-SBRs must thus be implemented in the CFAS system. Several designs have been reported that do employ selective wasting to retain granular sludge (Kent et al., 2018; Daigger et al., 2023), but do not maximize granular growth to the same extent as in bottom-fed SBRs. Selection for anaerobic storage of rbCOD and a macro-gradient of substrate in the mixed liquor to maximize penetration depth are used, but they are not coupled to selective feeding of the largest granular size class (van Dijk et al., 2022). Bioaugmentation with sludge from a side stream AGS-SBR has also been proposed as a strategy to increase the nitrogen removal performance of CFAS systems with a relatively low solids retention time (SRT) (Figdore et al., 2018; Miyake et al., 0000). No study thus far has investigated a direct translation of all relevant conditions from SBRs to CFAS systems in a mainstream application.

In addition, the quantitative comparison between the effectiveness of design considerations for aerobic granulation in CFRs has been hampered by the absence of a framework describing how process conditions affect growth of AGS in SBRs. The distribution of substrate has been shown to drive the development of the sludge particle size distribution in granular sludge reactors in general (Beeftink and van den Heuvel, 1990). For AGS specifically, the sensitivity analysis by van Dijk et al. (2022) showed that the mode of operation in the anaerobic phase of a SBR can have a large impact on granulation through the distribution of granule forming substrates (GFS). Heterotrophic microorganisms utilize GFS as a carbon source, storing it as intracellular polymers. Non-GFS are organic compounds that cannot diffuse into granules or are hardly converted to storage polymers, and therefore lead to flocculent growth that hinders granule formation (Layer et al., 2019). Three mechanisms impact the anaerobic distribution of GFS: microbial selection for anaerobic storage of GFS, maximizing diffusive substrate transport into granules, and selective feeding of large granules. Both selective and non-selective anaerobic substrate distribution could drive granulation on synthetic wastewater with only GFS (Haaksman et al., 2023). Using selective feeding to maximize granular growth is more critical for real wastewater when a substantial part of the COD consists of non-GFS (Layer et al., 2019; Rocktäschel et al., 2013), and requires further investigation.

In this study, a pilot-scale CFR was developed to best mimic the implementation of the granulation mechanisms of full-scale AGS-SBRs proposed by van Dijk et al. (2022). Selective feeding and selective wasting drive granulation through the targeted growth and retention of granular sludge, respectively. The reactor was fed with pre-settled municipal wastewater from the Harnaschpolder WWTP (The Netherlands). We established metrics to assess the degree to which the proposed mechanisms were implemented in the pilot-scale CFR and compared them to data from AGS-SBRs. To further study the impact of anaerobic substrate distribution on the growth of AGS, the pilot-scale CFR was also operated with a completely mixed anaerobic stage typical for CFAS systems employing EBPR.

2. Methodology

2.1. Description of the Harnaschpolder WWTP

The pilot-scale research was conducted at the Delft Blue Innovations research facility (Delfluent Services, Evides Industriewater and the Delfland Water Authority, 2022) at the Harnaschpolder WWTP in The Netherlands (52°0′59.724″N, 4°19′4.4076″E). The WWTP was designed for a capacity 1.26 million people equivalents (1 p.e. = $150\,mg_{COD}\,d^{-1}$) and a daily dry weather flow (DDWF) of $215\,000\,m^3\,d^{-1}$. Pre-settled influent is treated by the BNR-stage for removal of phosphorus, nitrogen and COD according to the PhoSim-process (van Nieuwenhuijzen et al., 2008).

2.2. Description of the pilot-scale CFR

The design of the pilot-scale reactor was set-up as a translation from an AGS-SBR to an equivalent CFR. Each research period was started by seeding AGS from a full-scale SBR at the Utrecht WWTP (The Netherlands). This approach was chosen to directly study the effect of the design and operation of the pilot-scale CFR on all mechanisms affecting the sludge morphology (van Dijk et al., 2022). The reactor was sized to operate at the same average SRT as the CFAS system of the Harnaschpolder WWTP (20 d), while maintaining an MLSS concentration of $8\,g_{TSS}\,L^{-1}$ of granular sludge. The volumetric loading rate of the pilot-scale CFR at DDWF was therefore increased twofold compared to the Harnaschpolder WWTP designed for a MLSSS concentration of $4\,g_{TSS}\,L^{-1}$ of AS (i.e. from 1.04 to $2.08\,m^3_{influent}\,m^{-3}_{reactor}\,d^{-1}$).

An overview of the pilot-scale CFR is depicted in Fig. 1. Influent was continuously supplied to the reactor at a constant flow rate of 0.5 $m^3 h^{-1}$. The flow rate was set to the average DDWF volumetric loading rate of the Harnaschpolder WWTP. The reactor therefore received a lower loading during rain weather flow (RWF) due to dilution of the wastewater. The WWTP receives a peak RWF flow rate of 35 800 $m^3 h^{-1}$. An electrical conductivity sensor in the influent supply was used to monitor the decrease in strength of the wastewater during RWF, based on which the sludge production was estimated, and the interval of excess sludge removal adjusted accordingly. The influent was directed to the anaerobic stage (Section 2.3.1). The mixed liquor then flowed to the subsequent stage of six tanks in series. Each tank had a working volume of 1 m^3 that could be mechanically mixed, mixed through fine bubble aeration, or both. The airflow to each tank was controlled from 0.42 mm s^{-1} to 1.04 mm s^{-1} via a valve. The last of the tanks in series was equipped with a manifold used for batchwise selective wasting, submerged at a depth of 35 cm. The flow to the last tank (C6) and the mechanical mixing were intermittently stopped to allow for the sludge to settle for a preset period of time, after which the mixed liquor above the manifold was discharged to an excess sludge buffer. During normal operation between waste sludge discharge events, the mixed liquor flowed from the last tank to the final clarifier (cone shaped) with a surface loading rate of 1.39 m h^{-1}. Thickened sludge was returned to the anaerobic stage via a peristaltic pump. Another pump of the same model was used to pump NO_x-rich mixed liquor from last aerated (C5) tank to the first anoxic tank acting as a pre-DN zone (C1). The reactor performance was monitored and controlled via on-line sensors.

2.3. Anaerobic stage configurations

2.3.1. Two alternating anaerobic upflow selectors (period I)

The anaerobic stage was designed based on an analysis of AGS-SBRs with respect to aerobic granulation (van Dijk et al., 2022). For the same wastewater, the anaerobic distribution of substrate over the granule size classes could be kept the same if the same superficial liquid velocity would be applied to expand a sludge bed. This would ensure a similar amount of bed expansion, degree of stratification over the height and degree of axial dispersion, which in turn would yield the same anaerobic substrate distribution. Second, the anaerobic residence time of the sludge in the CFR should be the same as the duration of the anaerobic feeding phase in the SBR.

A continuous anaerobic stage with two upflow selectors (Fig. 1) was designed to achieve this. Each selector was operated as an anaerobic SBR in an alternating fashion. While either one of the upflow selectors was receiving the influent, the return sludge flow was directed to the other selector. A working height of 2.5 m was chosen to allow for the accumulation of the same settled bed height as in the reference SBR (Pronk et al., 2015). Each upflow selector had a conical bottom with a slope of 60° that was used to displace saturated sludge to the first anoxic tank after the feeding phase. Influent was fed via a pipe directed at the bottom of the cone. Return sludge was added at a height of 1.5 m. Mixed liquor could overflow through an outlet at the top of the selector to first anoxic tank. A cycle of an anaerobic upflow selector consisted of the following phases (see Fig. 1):

1. *Displacement phase*: return sludge was added to selector A at 1.5 m and was allowed to settle on to the top of the remaining sludge bed after anaerobic feeding. The sludge saturated with storage polymers at the bottom of the bed was simultaneously displaced through the bottom outlet to first anoxic tank.
2. *Accumulation phase*: after the complete volume of the sludge bed in upflow selector A had been displaced by granular sludge from the return sludge, the withdrawal of sludge at the bottom was stopped. The supply of return sludge was continued for the accumulation of granular sludge on top of the bed, if the sludge could settle faster than the applied superficial upflow velocity. Sludge size classes with a too low settleability overflowed at the top of the selector towards the anoxic tank and effectively bypassed the anaerobic stage.
3. *Feeding phase*: once the feeding phase in selector B had finished, the flow of influent was directed to selector A. The flow of return sludge was simultaneously switched to upflow selector B. The sludge bed in selector A would then expand due to applied superficial liquid velocity. Sludge size classes with insufficient settleability would wash out of the expanded bed and overflow at the selector. Furthermore, the sludge size classes that remained in the expanded bed would stratify from top to bottom with increasing settleability. Once the feeding phase in selector A had finished, the cycle was restarted.

2.3.2. Mixed anaerobic selector and anaerobic tank (control, period II)

To investigate the contribution of the upflow selectors to the growth of AGS, the anaerobic stage was altered during the control period to resemble that of the full-scale CFAS system at the Harnaschpolder WWTP Fig. 1. It consisted of a completely mixed anaerobic selector compartment with a mixed liquor residence time of 16 min, followed by a completely mixed anaerobic compartment (C1) with a residence time of 1 h. The return sludge was directed partly to the anaerobic selector (45%) and partly to the second anaerobic tank (55%). The complete flow of influent was directed to the anaerobic selector. The residence time distribution was the same for all sludge size classes due to mechanical mixing, regardless of differences in settleability. The anaerobic distribution of GFS was determined only by the kinetics of mass transfer and biological conversions. This removed the selective advantage for the best-settling granular sludge size classes over flocculent sludge in the anaerobic distribution of GFS (Haaksman et al., 2023), reducing this selective pressure for aerobic granulation compared to the anaerobic upflow selectors. The average sludge loading of GFS in the anaerobic stage was similar to period I.

2.3.3. Control of nutrient removal

Compartments C2 till C5 of the tanks in series served as an aerobic zone. Compartments C2 and C3 were continuously aerated and the airflow was regulated to maintain a setpoint for the dissolved oxygen concentration between 1–2 mg L^{-1}. The airflows to compartments 4 and 5 were controlled to limit the concentration of nitrate in the effluent (and return sludge) to a maximum of 10 mg NO_3^--N L^{-1}. If the ammonium concentration in the effluent came below 1 mg NH_4-N L^{-1}, the airflows to compartments C4 and C5 were lowered to achieve maximum simultaneous denitrification.

NO_x-rich mixed liquor was recycled from the last aerated compartment (C5) to the first anoxic tank (C1) for pre-denitrification (Fig. 1). The ratio of the recycle flow rate compared to the flow of influent was between 1 and 2 $m^3_{ML}\ m^{-3}_{influent}$.

2.3.4. Discharge of excess sludge (selective wasting)

Excess sludge was discharged through a submerged manifold in the last compartment of the tanks in series (C6), prior to the final clarifier (Fig. 1). A batchwise procedure was used to perform selective wasting of sludge based on a settling speed criterion of 3.6 m h^{-1}, within the range of superficial upflow velocities used in Nereda® reactors (van Dijk et al., 2018). The flow to the last compartment was stopped and the mechanical mixer was turned off, after which the sludge was allowed to settle. After a preset time the outlet valve was opened, and the excess sludge was discharged. Operation would continue as normal until the next discharge cycle. The interval between discharge cycles was set to maintain a sludge volume after five minutes of settling (SV_5) of 400–500 mL mL^{-1}_{ML}.

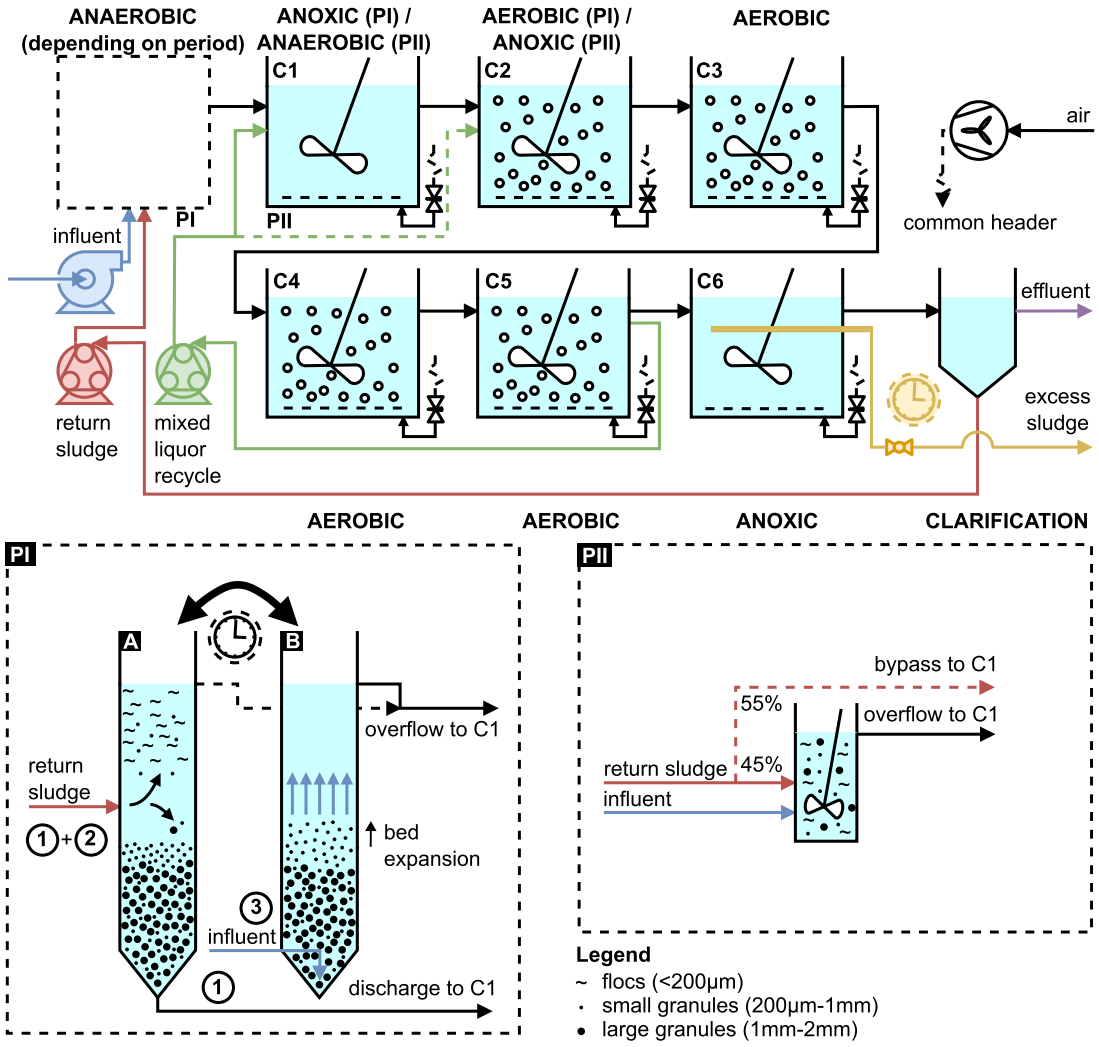

Fig. 1. (top) Schematic overview of the pilot-scale continuous flow reactor. The differences between the configuration during trial period 1 and trial period 2 are indicated via PI en PII, respectively. (bottom) Detailed description of the anaerobic stages of the pilot-scale CFR during the two operational periods. (bottom left) Period I (PI): two alternating upflow selectors based on the anaerobic phase of a SBR employing AGS. The numbers in the image refer to the numbering of the phases of an anaerobic feeding cycle described in Section 2.3.1. (bottom right) Period II (PII): an anaerobic selector followed by a larger anaerobic tank (both completely mixed) that resembled after the anaerobic stage of the Harnaschpolder WWTP. Acronyms: AO: anoxic compartment, AN: anaerobic compartment.

2.4. Analytical procedures

Concentrations of compounds in mixed liquor samples were determined via analysis kits from the LCK-system and a DR3900 spectrophotometer from HACH (Loveland (CO), USA). Samples were prepared using 0.45 µm Puradisc AQUA syringe filter from Whatman (Marlborough (MA), USA). The concentration of acetate was determined by high-performance liquid chromatography (HPLC) with an Aminex HPX-87H column from Bio-rad (Hercules (CA), USA), coupled to an UV detector, using 0.01 M phosphoric acid as the eluent. Samples for HPLC were filtered through a 0.2 µm PVDF-membrane from Whatman (Marlborough (MA), USA).

Mixed liquor suspended solids (MLSS) concentrations, volatile suspended solids (MLVSS) concentrations and sludge volume indices after 5 min and 30 min were determined according to Van Loosdrecht et al. (2016). The size class distribution of a sludge sample was determined by first pouring the sample over a stack of sieves with decreasing mesh size and rinsing each sieve with tap water.

Samples for characterization of the sludge morphology were transferred to a glass petri dish and examined with an Olympus reverse microscope (Shinjuku (Tokyo), Japan) with a Leica digital camera (Wetzlar, Germany).

2.5. Specific activities of sludge size classes

2.5.1. Anaerobic uptake rate and storage capacity of GFS

The maximum anaerobic conversion rate of GFS and the capacity for storage as intracellular polymers were determined via batch tests using acetate. A mixed liquor sample was taken from the return sludge, prior the anaerobic stage. If the sludge was fractionated using sieves, each fraction was recombined with filtered effluent (7 µm). In either case, the initial volume was 840 mm with an approximate MLSS concentration of 2 $g_{TSS}\,L^{-1}$, containing a 10 $\mu mol\,L^{-1}$ HEPES-buffer to ensure a stable pH of 7. The temperature was kept constant at 20 °C. Oxygen was first stripped from the liquid by sparging dinitrogen gas at a rate of 1 $L\,min^{-1}$, which continued throughout the experiment. The experiment was started via the addition of 10 mL of a solution of 42.5 $g_{Ac^-}\,L^{-1}$ to reach an initial concentration of 500 $mg_{Ac^-}\,L^{-1}$. This set-up was developed to achieve complete penetration of acetate of in the largest granule size class within 5 min and to allow sampling in the zero-order kinetics range during the first 60 min of the experiment (Haaksman et al., 2023). The loading was sufficient to achieve saturation of the storage capacity. Samples of 10 mL were taken every 10 min during to 60 min and immediately filtered through a 0.45 µm Puradisc AQUA filter from Whatman (Marlborough (MA), USA) and stored at 4 °C for

Table 1
Characteristics of the pre-settled municipal wastewater of the Harnaschpolder WWTP over a time period of one year.

Component (unit)	Influent concentration
N_{Kj} ($mg_N\,L^{-1}$)	57.4 ± 7.8
P_{total} ($mg_P\,L^{-1}$)	9.3 ± 1.4
PO_4^{3-} ($mg_P\,L^{-1}$)	6.8 ± 0.9
COD ($mg_{O_2}\,L^{-1}$)	503 ± 84
$COD_{<0.45\,\mu m}$ ($mg_{O_2}\,L^{-1}$)	257 ± 38
COD_{VFA} ($mg_{O_2}\,L^{-1}$)	109 ± 32
inert $COD_{<0.45\,\mu m}$ ($mg_{O_2}\,L^{-1}$)[a]	29
$COD_{<0.45\,\mu m}$ converted anaerobically (%)[b]	40 to 60

[a] Equal to the average concentration of $COD_{<0.45\,\mu m}$ in the effluent of the CFR.
[b] Estimated according to Section 2.5.1.

analysis. A final sample was taken after 150 min to determine total storage capacity through the remaining concentration of acetate. All biomass in each container was subjected to the determination of the MLSS and MLVSS at the end of the experiment.

2.5.2. Fraction of GFS in the influent

The maximum fraction of $COD_{<0.45\ \mu m}$ in the pre-settled municipal wastewater available for anaerobic storage was estimated from batch tests with the influent combined with return sludge. The size of 0.45 μm has been reported to be close to the cut-off point for particles to be diffusible into granules (van den Berg et al., 2022), and was therefore used as proxy for GFS. The ratio of influent to return sludge in the test was set to obtain a COD loading ($mg_{O_2}\,g_{TSS}^{-1}$) such that the anaerobic storage capacity of the sludge was not exceeded. The batch tests were conducted in the same way as described in Section 2.5.1.

2.5.3. Aerobic conversion rates

The maximum specific aerobic conversion rates for simultaneous removal of ammonium (SNUR) and phosphate (SPUR) were determined via batch tests. A mixed liquor sample was taken from the end of the anaerobic stage. The sludge was either thickened through settling and decanting, or the sludge was fractionated into size classes using sieves. In both cases, the sludge was recombined with filtered mixed liquor (7 μm) from the end of the anaerobic stage. The initial volume was 840 mm with an approximate MLSS concentration of $3\,g_{TSS}\,L^{-1}$, containing a $10\,\mu mol\,L^{-1}$ HEPES-buffer to ensure a stable pH of 7. The temperature was kept constant at 20 °C. The experiment was initiated by starting the supply of oxygen via sparging of air at a rate of $1\,L\,min^{-1}$ and ensured saturation of the liquid with dissolved oxygen. This set-up was developed to allow sampling in the zero-order kinetics range during the first 60 min of the experiment. Samples of 10 mL were taken every 10 min during to 60 min. The sample processing and the remainder of the experiment were performed according to 2.5.1.

3. Results

The pilot-scale CFR was fed with pre-settled municipal wastewater of the Harnaschpolder WWTP as influent. The characteristics of the pre-settled wastewater are listed in Table 1. Each of the two research period was started by seeding AGS from a full-scale SBR. The initial MLSS concentration was between 6–8 $g_{TSS}\,L^{-1}$. If conditions for granular growth were inadequate, the granular sludge fraction would decrease rapidly after seeding. If the AGS grew and maintained its morphology after seeding, it indicated favorable conditions for granular sludge formation.

3.1. Seed sludge characteristics

The seed sludge originated from an AGS-SBR at Utrecht WWTP (The Netherlands) designed for biological removal of nitrogen, phosphorus and COD, similar to the reactor described by Pronk et al. (2015). The granule size distribution of the seed sludge is listed in Table 2. The morphology of seed sludge is depicted in Fig. 2(a). The size class <200 μm consisted of compact flocs, while the class from 200–400 μm contained cellulose and granular nuclei. Small (400–1000 μm), medium (1000–2000 μm) and large granules (>2000 μm) shared a similar smooth morphology with limited surface outgrowth. The shape of the granules did show a decrease in sphericity with increasing size. The average ratio of VSS/TSS was 80%.

Table 2
Size distribution of the seed sludge from an AGS-SBR at Utrecht WWTP (The Netherlands) used for the pilot-scale CFR.

Size class	MLSS ($g_{TSS}\,L^{-1}$)	Relative contribution
<200 μm	1.85	22%
200–400 μm	0.28	3%
400–1000 μm	0.89	11%
1000–2000 μm	2.47	29%
>2000 μm	2.96	35%

3.2. Period I: two alternating anaerobic upflow selectors

The anaerobic upflow selectors had to be operated such that the three mechanisms for the anaerobic distribution of GFS were implemented similarly to an AGS-SBR: microbial selection for anaerobic storage of GFS, maximizing transport of substrate into the granules and selective feeding of largest granules. Based on the modeling procedure from van Dijk et al. (2022), a superficial feeding velocity of $3.6\,m\,h^{-1}$ with an anaerobic feeding time of 1.5 h (average time to saturation of the anaerobic storage capacity, see Section 2.5.1) was expected to yield an anaerobic distribution of GFS similar to a full-scale AGS-SBR (Pronk et al., 2015; van Dijk et al., 2020). Using the maximum anaerobic conversion rate of GFS from the AS from Harnaschpolder WWTP, it was estimated that an expanded bed height of 1.2 m of granules >1 mm was required for complete anaerobic removal of GFS from the pre-settled influent.

After a trial period of 44 d during which the process control of the anaerobic upflow selectors (Fig. 1) was tested with a small amount of AGS, the CFR was seeded to approximately $8\,g_{TSS}\,L^{-1}$. The initial granular sludge mass fraction (>200 μm) was 78%, with 64% > 1 mm and 35% > 2 mm (see Fig. 3(a)). The MLSS concentration decreased slightly during the first two days, mainly due to the loss of the granules in the size class >2 mm. This was likely caused by disintegration due to the exposure to increased shear stress from the mechanical mixing and recycle pumps in the CFR, compared to only fine bubble aeration in the full-scale SBRs to which the seed sludge had been accustomed (van Dijk et al., 2020).

3.2.1. Sludge characteristics

The mass distribution and sludge properties stabilized after the initial seeding and were maintained during 166 days, after which the experiment was terminated. The average MLSS concentration was 6.4 ± 0.7 $g_{TSS}\,L^{-1}$ with a VSS/TSS ratio of 79%. The average size of granules (>200 μm) was 1.34 mm and the mass fraction of all granular sludge size classes was 66% (see Fig. 3(a)). The variation of the MLSS distribution over time observed in the pilot-scale CFR is common for AGS reactors treating sewage (Van der Roest et al., 2016).

The sludge settleability was stable throughout period I with an average SVI_{30} of 51 ± 6 $mL\,g_{TSS}^{-1}$ and a SVI_5/SVI_{30} ratio of 1.65 ± 0.1, which were comparable to values reported for full-scale AGS-SBRs (1.56, Pronk et al., 2015). The $dSVI_{30}$ of the AS from the full-scale CFAS system at Harnaschpolder WWTP averaged $100\,mL\,g_{TSS}^{-1}$ during the same period.

Visual inspection showed that the morphology of the granular sludge remained smooth throughout period I, based on the absence of filamentous or finger-type outgrowth (Pronk et al., 0000). Parts of the granular surfaces were occupied by stalked ciliates (see Fig. 2(b)).

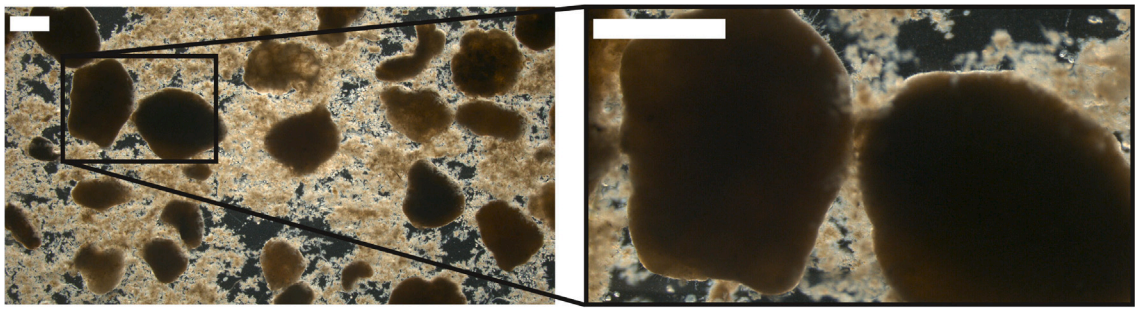

(a) Seed sludge from an AGS-SBR at Utrecht WWTP (The Netherlands).

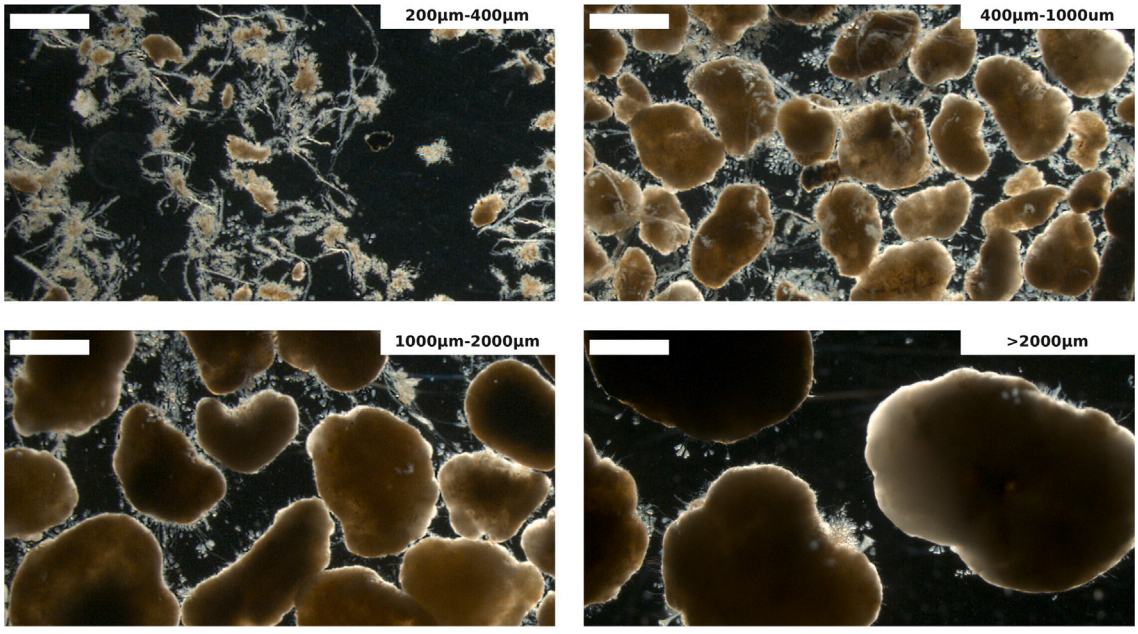

(b) Sieved fractions of sludge from the end of period I (after 166 days of operation) using two alternating upflow selectors.

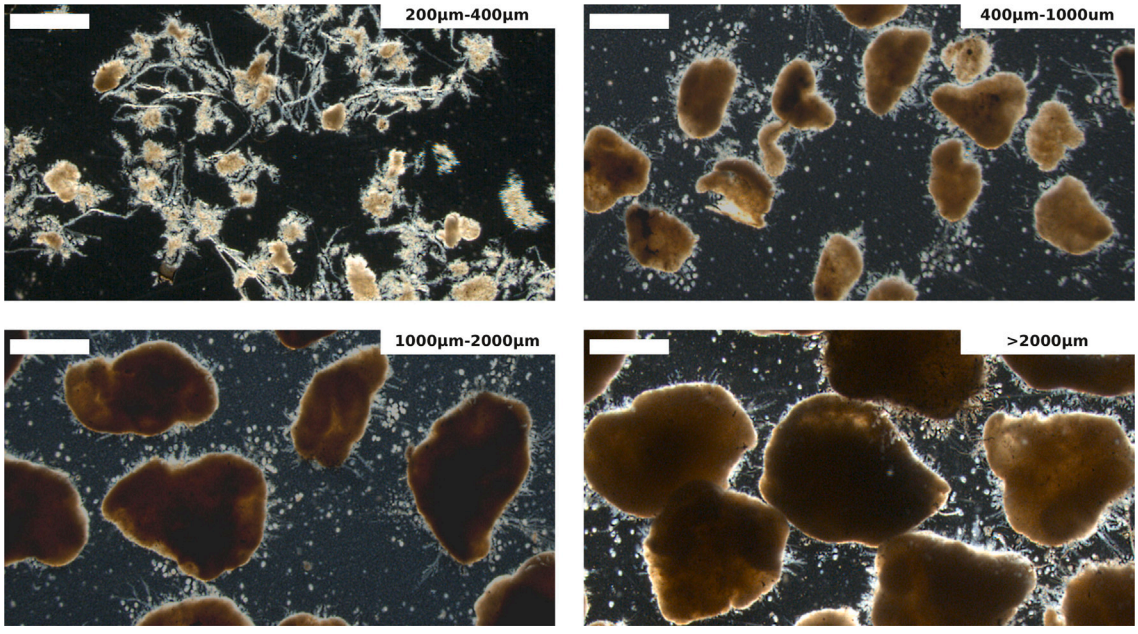

(c) Sieved fractions of sludge from the end of period II (after 129 days of operation) using a completely mixed anaerobic selector and subsequent anaerobic tank.

Fig. 2. Morphology of aerobic granular sludge size classes, fractionated using sieves and imaged via stereoscopic microscopy. The scale bar represents a length of 1 mm.

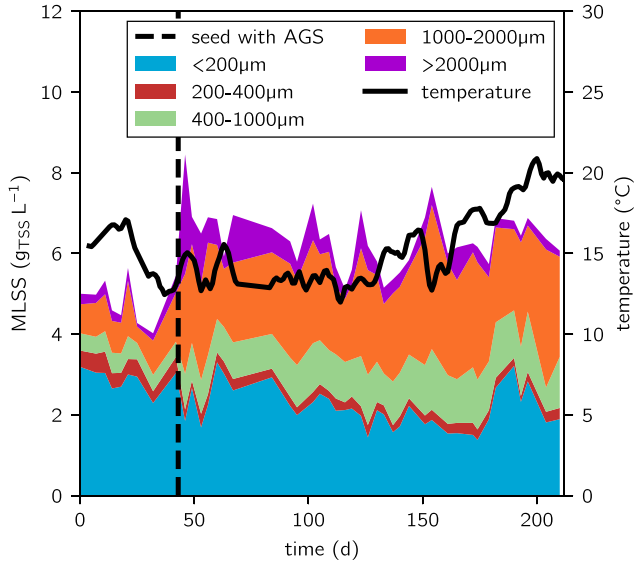

(a) Two alternating anaerobic upflow selectors (period I). The vertical line (black, dashed) indicates the time of seeding with aerobic granular sludge.

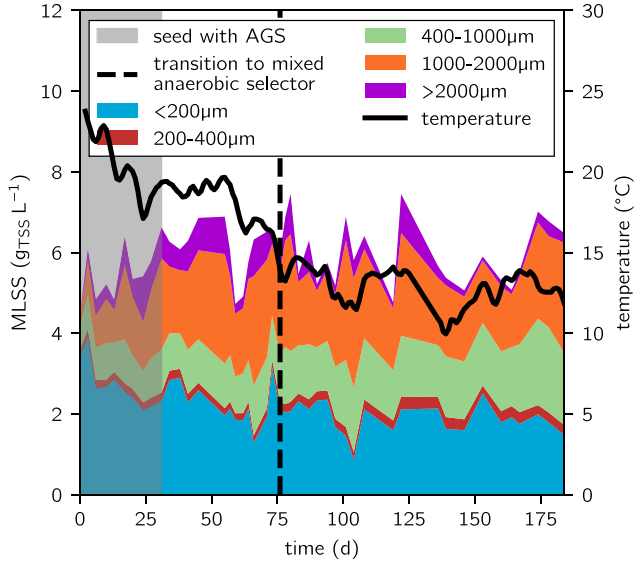

(b) Mixed anaerobic selector and anaerobic tank (period II). The vertical line (black, dashed) indicates the transition to the mixed anaerobic stage. The shaded area (grey) denotes the period during which aerobic granular sludge was seeded.

Fig. 3. Total MLSS and mass distribution over sludge particle size classes, and the temperature profile during the operational periods.

3.2.2. Anaerobic loading distribution

The extent to which the selective pressures for aerobic granulation were implemented were analyzed based on the framework proposed by van Dijk et al. (2022). The quantitative metrics for the mechanisms are listed in Appendix A.

All COD available for anaerobic conversion (GFS) was removed in the selector, ensuring microbial selection for anaerobic storage. This was determined from the removal of $COD_{<0.45\ \mu m}$ in the overflow during DWF, shown in Table 3. The anaerobically removable $COD_{<0.45\ \mu m}$ fraction in the influent ranged from 40–60%, which was considered to be the fraction of GFS (Table 1). The anaerobically removable $COD_{<0.45\ \mu m}$ consisted of volatile fatty acids and a fermentable fraction of COD. The removal efficiency of $COD_{<0.45\ \mu m}$ in the anaerobic upflow selector was 49%. Therefore, the amount of GFS in the influent was completely

Table 3
Characteristics for the anaerobic conversions for one of the alternating upflow selectors at the end of the anaerobic feeding phase (period I).

Component (unit)	Influent	Outflow of anaerobic upflow selector (removal)
COD ($mg_{O_2}\ L^{-1}$)	579	–[a]
$COD_{<0.45\ \mu m}$[b] ($mg_{O_2}\ L^{-1}$)	273	138 (49%)
COD_{VFA}[c] ($mg_{O_2}\ L^{-1}$)	115	<5 (>96%)
NH_4^+ ($mg_N\ L^{-1}$)	48.6	47.8
PO_4^{3-} ($mg_P\ L^{-1}$)	6.5	58.8

[a] Could not be determined since the overflow of the upflow selector contained substantial amounts of flocculent sludge.
[b] Corrected for the inert fraction of $COD_{<0.45\ \mu m}$, based on the amount in the effluent of the CFR (see Table 1).
[c] Combined value for all volatile fatty acids detected (i.e. acetate and propionate).

removed in the selector. The uptake of $COD_{<0.45\ \mu m}$ was coupled to the release of phosphate with an average P/COD-ratio of 0.39

The degree of plug-flow was investigated by measuring the residence time distribution (RTD, see Fig. 4). A cumulative RTD was determined by first expanding and stratifying the accumulated sludge in the upflow selector with effluent, followed by a normal feeding phase with influent. The concentration of ammonium in the overflow was used as a step-tracer. This concentration was normalized using the concentration of ammonium in the influent and the effluent, and fitted to an 1D axial dispersion model (Appendix A) which yielded an axial dispersion coefficient D_{ax} of $0.8\times10^{-4}\ m^2\ s^{-1}$. Therefore, the Péclet-number for the expanded bed in the upflow selector (Pe_B) was 13. An axial dispersion coefficient in the same order of magnitude has been reported for full-scale AGS-SBRs (i.e. $1\times10^{-4}\ m^2\ s^{-1}$, van Dijk et al., 2018) and the flow was characterized by a similar Péclet-number of 14. The upflow selector of the pilot-scale CFR thus exhibited a degree of plug-flow similar to a full-scale AGS-SBR.

To analyze the extent of selective feeding, the accumulation of granular size classes in the expanded bed during the feeding phase were compared to their mass fractions in the return sludge (Appendix A). This comparison served as a metric for the likelihood of these particles being retained in the anaerobic upflow selector (see Fig. 5). The average concentrations of sludge particles from a size class in the expanded bed were compared to the hypothetical maximum accumulated mass. While for the size class <400 µm only <10% had been retained at the end of the feeding phase, the retention probability increased with increasing particle size up to 90% for granules >2 mm. Most of the biomass (85%) fell in the size class >1 mm and the total MLSS concentration was 40 $g_{TSS}\ L^{-1}$ (Fig. 5), and the average expanded bed height at the end of the feeding phase was 105 ± 13 cm, both as intended.

The upflow selectors imposed a non-uniform distribution of the anaerobic retention time due to wash-out of smaller size classes through the overflow (Fig. 5). While all sludge in a completely mixed anaerobic stage has the same residence time, a below average anaerobic retention time was imposed on the flocculent sludge (<200 µm) and the smallest granule size class (200–400 µm). Granules in the size classes >1000 µm experienced an above average residence time. A reversed trend was observed for the residence time in the aerobic/anoxic stages.

3.2.3. Selective discharge of excess sludge

The effect of selective wasting was assessed by comparing the mass fractions of different size classes in the discharged sludge with those in the MLSS (see Fig. 6(a)). While the sludge <400 µm had a retention probability of 55%, all granular size classes >400 µm were almost completely retained with probabilities >90%.

The observed retention probabilities were used to calculate the overall SRT of each size class for comparison with the average overall SRT of 18 ± 4 d. Sludge in size classes <400 µm had a below average SRT shorter than 10 d, while the granular size classes >1 mm exhibited

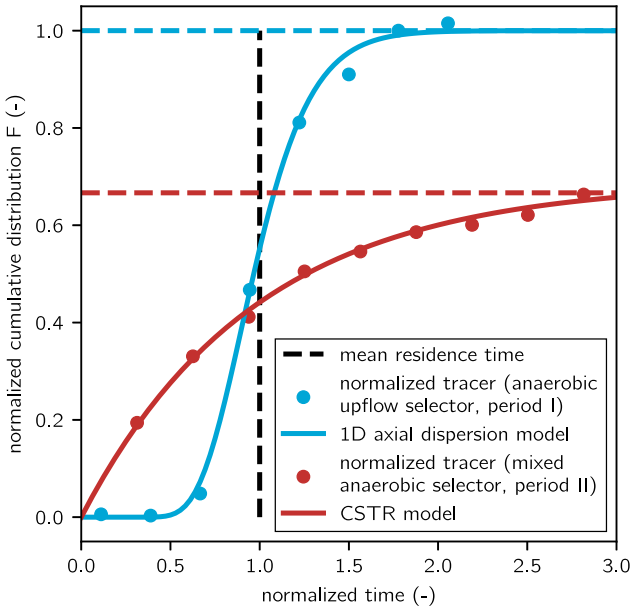

Fig. 4. Normalized cumulative RTD for the feeding phase of an anaerobic upflow selector used in the CFR during period I (solid spheres, blue) and the anaerobic selector used in period II (solid spheres, red). The normalized variances (σ^2) were 0.07 and 0.81, respectively. The normalized concentrations were fitted to a transient 1D axial dispersion model with an axial dispersion coefficient (D_{ax}) of $0.8\times10^{-4}\,m^2\,s^{-1}$ for period I (solid line, blue), and to a single CSTR-model for period II (solid line, red). The horizontal lines (dashed) depicts the reduced maximum concentration in the completely mixed anaerobic selector relative to the influent due to the dilution by the return sludge flow in period II (red), while this was not the case for the anaerobic upflow selector in period I (blue). (For interpretation of the references to color in this figure legend, the reader is referred to the web version of this article.)

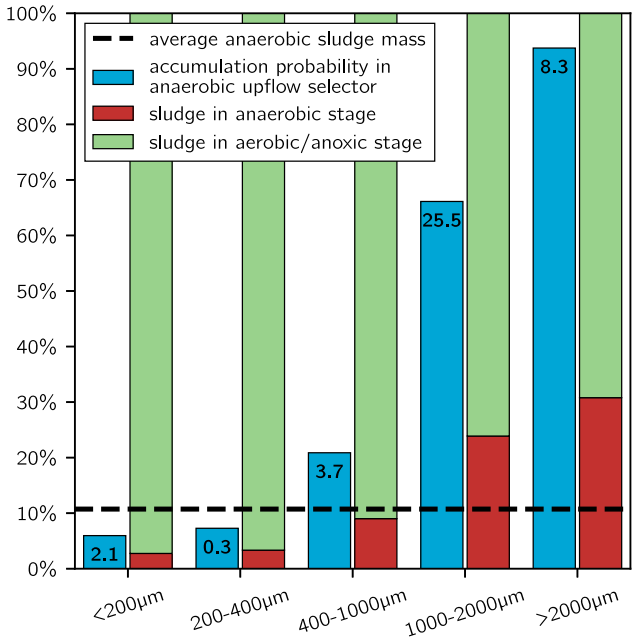

Fig. 5. The selective anaerobic retention probability of sludge is depicted, as a function of granule size class in an anaerobic upflow selector (blue bars). The numbers (black) above the bars denote the average MLSS concentration ($g_{TSS}\,L^{-1}$) of a size class in the expanded bed. The residence time distribution of sludge over either the anaerobic upflow selectors (red bars) or the combined aerobic/anoxic volume (including the final clarifier, green bars) is shown as function of the size class. The theoretical average anaerobic residence time (dashed) was calculated based on the working volume of the anaerobic stage relative to the aerobic/anoxic stage, for the case with a completely mixed anaerobic stage where all sludge was uniformly distributed over the volume. (For interpretation of the references to color in this figure legend, the reader is referred to the web version of this article.)

SRTs more than one order of magnitude larger than the average SRT. The same increasing trend was observed in the SRT distribution of size classes as in the selective wasting of excess sludge.

3.3. Period II: mixed anaerobic selector and anaerobic tank

The configuration of the CFR was altered during period II to resemble the completely mixed anaerobic stage of the CFAS system of Harnaschpolder WWTP (Fig. 1). The CFR was again seeded with sludge from the Utrecht WWTP to start the experiment with a similar granular sludge distribution as in period I (Fig. 3(b)). The seeding took place over the course of one month due to a more dilute shipment of AGS used for seeding, which complicated the transfer to the CFR. The reactor was operated with the upflow selectors as anaerobic stage to allow the sludge to adjust for approximately four average SRTs (day 76), after which the configuration of the anaerobic stage was transitioned to the mixed compartments. The average loading of the sludge in the anaerobic stage with $COD_{<0.45\ \mu m}$ was $10\,mg_{O_2}\,g_{TSS}^{-1}$, similar to period I.

3.3.1. Sludge characteristics

Stable sludge properties were maintained after transitioning to the mixed anaerobic stage over the course of 108 days (Fig. 3(b)). The average MLSS concentration was $6.0 \pm 0.8\,g_{TSS}\,L^{-1}$ with a VSS/TSS ratio of 81%, and the average granular mass fraction (>200 µm) was 68%. Compared to period I, the mass distribution had shifted down from the 1000–2000 µm size class to the 400–1000 µm size class. This decreased the average granule diameter slightly to 1.28 mm.

The sludge settleability was stable throughout the whole operational period with an average SVI_{30} of $53 \pm 7\,mL\,g_{TSS}^{-1}$ and a SVI_5/SVI_{30} ratio of $1.76 \pm 0\,1$, which were both slightly higher than during period I. The $dSVI_{30}$ of the activated sludge from Harnaschpolder WWTP remained on average $100\,mL\,g_{TSS}^{-1}$.

The smoothness of the granular surfaces did not show major differences compared to period I.

3.3.2. Anaerobic loading distribution

Complete removal of the COD_{VFA} was achieved in the combined anaerobic selector and subsequent anaerobic tank Table 4, part of the total fraction of 59% of $COD_{<0.45\ \mu m}$ that was removed. This was similar to the anaerobic upflow selector used in period I and within range of the fraction of $COD_{<0.45\ \mu m}$ from the influent that was anaerobically removable and considered the fraction of GFS (Table 1). The COD removed in the anaerobic selector was mainly COD_{VFA} and was coupled to a higher P/COD-ratio than in the subsequent anaerobic tank, although the average P/COD-ratio for both anaerobic tanks was 0.34, similar to period I.

The cumulative RTDs of the anaerobic selector and subsequent anaerobic tank in series were determined using the same method as used for the anaerobic upflow selectors. The residual concentration of GFS in the completely mixed anaerobic selector was lower than the influent concentration due to the mixing of influent and (part of) the return sludge. This lowered the maximum substrate penetration depth compared to the anaerobic upflow selectors (Fig. 4).

The RTD of the anaerobic selector was measured to compare the extent of selective feeding. All sludge was kept in suspension via the mechanical mixing, and therefore the RTD of all sludge size classes were the same. The residence time for the largest granules in the expanded bed in an upflow selector during period I was 1.5 h (i.e. equal to the duration of the feeding phase) and continuously in contact with fresh influent. On the other hand, the average residence time of all the sludge in the anaerobic selector was 16 min. The mean residence time of the subsequent anaerobic tank was longer (i.e. 66 min). The

Table 4
Characteristics anaerobic conversions for the mixed anaerobic selector and the subsequent anaerobic tank (period II). All values were scaled to account for dilution of the influent by the return sludge flow (45% to the anaerobic selector, 55% to the subsequent anaerobic tank) to allow for mutual comparison.

Component (unit)	Influent	Anaerobic selector (removal)	Anaerobic tank (removal)
COD ($mg_{O_2}\ L^{-1}$)	497	–[a]	–[a]
$COD_{<0.45\,\mu m}$[b] ($mg_{O_2}\ L^{-1}$)	250	189 (24%)	102 (59%)
COD_{VFA}[c] ($mg_{O_2}\ L^{-1}$)	112	51 (54%)	<5 (>96%)
NH_4^+ ($mg_N\ L^{-1}$)	51	50.8	52.4
PO_4^{3-} ($mg_P\ L^{-1}$)	6.7	39.2	51.7

[a] Could not be determined since particulate COD was mixed with MLSS.
[b] Corrected for the inert fraction of $COD_{<0.45\,\mu m}$, based on the amount in the effluent of the CFR (see Table 1).
[c] Combined value for all volatile fatty acids detected (i.e. acetate and propionate).

total mean anaerobic residence time was thus similar to period I, but the residual concentration of COD_{VFA} was close to zero in this second anaerobic compartment (Table 4). For equal contact time, the lower concentrations favor the uptake of substrate by biomass in smaller sludge particles with more specific area.

3.3.3. Selective discharge of excess sludge

The selective discharge of excess sludge was operated the same as during period I. The selective retention probabilities (Fig. 6(b)) were nearly identical to those observed for all size classes in period I. The SRT distribution was almost identical as well, except for the increase in average SRT for the size class (400–1000 μm) from 33 d to 51 d due to the increase in MLSS of this fraction (Fig. 3(b)). The SRT of the size class of 1000–2000 μm decreased from 429 d to 373 d. The differences in SRT distribution between periods I and II were relatively small compared to the shift in anaerobic distribution of GFS towards the flocculent sludge fraction (Section 3.3.2).

3.4. Biological treatment performance

3.4.1. Removal efficiencies and effluent quality

The nutrient removal performance of the CFR was analyzed for the last 30 days of period I for comparison with the full-scale CFAS system. The concentration of organic pollutants in the secondary effluent was <30 $COD_{<0.45\ \mu m}$ for both the full-scale CFAS system and the pilot-scale CFR. The removal efficiencies for phosphorus and nitrogen in the CFR were 97% and 84%, respectively. The overall volumetric removal rates were 15 $g_P\ m_{reactor}^{-3}\ d^{-1}$ and 98 $g_N\ m_{reactor}^{-3}\ d^{-1}$, which yielded average effluent concentrations of 0.3 $mg_{PO_4-P}\ L^{-1}$ and 9.9 $mg_{TN}\ L^{-1}$. The biological nutrient removal stage of Harnaschpolder WWTP, treating the same pre-settled wastewater, achieved similar removal efficiencies (i.e. 92% for phosphorus and 92% for nitrogen). The CFAS system reached a better effluent quality with respect to the total nitrogen concentration (i.e. 0.7 $mg_{PO_4-P}\ L^{-1}$ and 5.4 $mg_{TN}\ L^{-1}$). The overall volumetric removal rates of the full-scale CFAS system were 7 $g_P\ m_{reactor}^{-3}\ d^{-1}$ and 48 $g_N\ m_{reactor}^{-3}\ d^{-1}$. A more than twofold increase in both the volumetric phosphorus and nitrogen removal rates were achieved (at similar reactor temperatures of 17.5 ± 0.5 °C) with the AGS in the CFR compared to the full-scale CFAS system.

3.4.2. Biomass specific conversion rates per size class

To determine the specific conversion rates for both ammonium (SNUR, nitrification and growth) and phosphate (SPUR, EBPR and growth), aerobic batch tests were conducted on sieved sludge fractions at the end of both research periods (Fig. 7). The obtained rates were used to examine how the differences in the anaerobic stage between periods I and II impacted the distribution of microbial activity over the size classes, and how they compared to the AS of Harnaschpolder WWTP. Initial concentrations for ammonium and phosphate were the same as in the CFR and the liquid phase was saturated with oxygen to minimize mass transfer limitations. The obtained specific conversion rates were interpreted as the maximum that could be obtained under reactor conditions.

The SNUR for period I showed a decreasing trend with an increasing average diameter of the sludge size class (Fig. 7(a)). On the other hand, the SNURs of sludge <400 μm in the CFR were similar to that of the CFAS system. The rates showed a sharp decrease from the size class <1000 μm to >1 mm. The same experiment performed at the end of period II showed a similar, but more gradual decreasing trend for the SNUR with increasing particle size. Furthermore, the bandwidth between the highest rates (i.e. flocculent sludge fraction) and the lowest rates (i.e. largest granule size class) was smaller (Fig. 7(b)).

The SPUR for period I showed a different trend compared to the ammonium removal (Fig. 7(a)). For the size classes >400 μm the maximum specific rates were comparable, but they were substantially larger than the rate of the flocculent sludge fraction from the CFR. The maximum SPUR of the AS was 1.8-fold larger than the maximum rate observed in the pilot-scale CFR, while for ammonium removal the difference was negligible. The distribution in the SPUR between size classes showed a parallel with the retention probability of each class in the anaerobic upflow selectors (see Fig. 5). The flocculent sludge fraction (<200 μm) had a retention probability lower than the average retention without selective feeding and showed the lowest SPUR. On the other hand, the transition to an above average retention probability in the upflow selector for granules >400 μm coincided with the transition to a substantially larger SPUR compared to the flocculent fraction. The trend for the SPUR at the end of period II differed substantially from period I, showing an inverse trend with increasing particle size (Fig. 7(b)). The SPUR of the flocculent sludge in period II was 2.7-fold larger than those of the granular size classes (i.e. >400 μm).

3.4.3. Contributions to volumetric removal rates

Based on the specific nutrient removal rates per size class, the contribution of each class to the overall nutrient removal was estimated (see Fig. 8). The contribution of the flocculent fraction (<200 μm) to volumetric removal rate of ammonium was similar for both research periods and amounted to at least 50%. The remaining contributions from the granular sludge fractions showed similar trends for both periods as well. The contributions to the total volumetric phosphate removal rate did differ substantially between both periods. The granular sludge fractions >400 μm contributed 78% to the total volumetric rate during period I, while this was 30% in period II. The changes in anaerobic process conditions therefore caused relatively small changes in the MLSS-distribution over size classes between (Fig. 3), but induced relatively large shifts in the distribution of EBPR activity over the size classes.

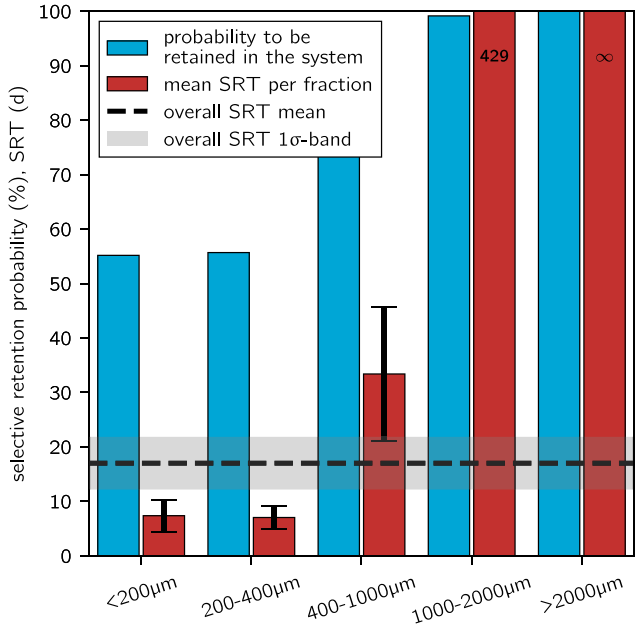

(a) Two alternating anaerobic upflow selector (period I).

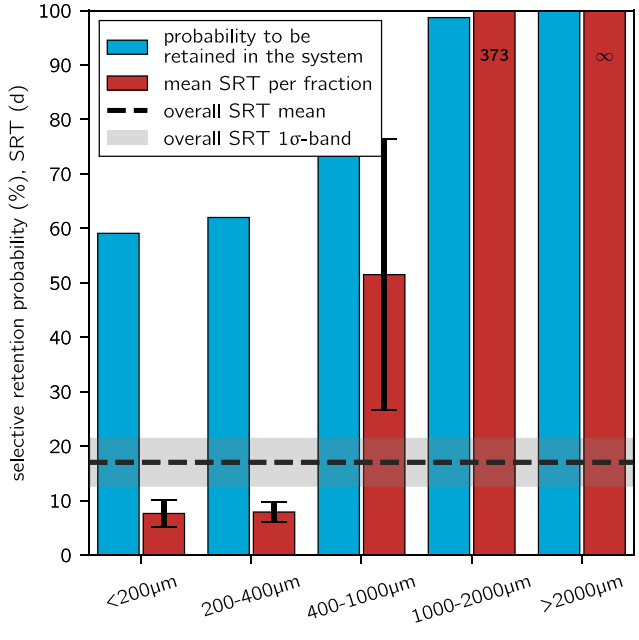

(b) Mixed anaerobic selector and anaerobic tank (period II).

Fig. 6. Selective retention probabilities of the different size classes of sludge particles (blue bars), SRT of individual size classes (red bars) and the weighted average SRT for the MLSS as a whole (dashed line). All error bars and error bands represent a distance 1σ from the respective means as an indication of the variability observed during the research period. (For interpretation of the references to color in this figure legend, the reader is referred to the web version of this article.)

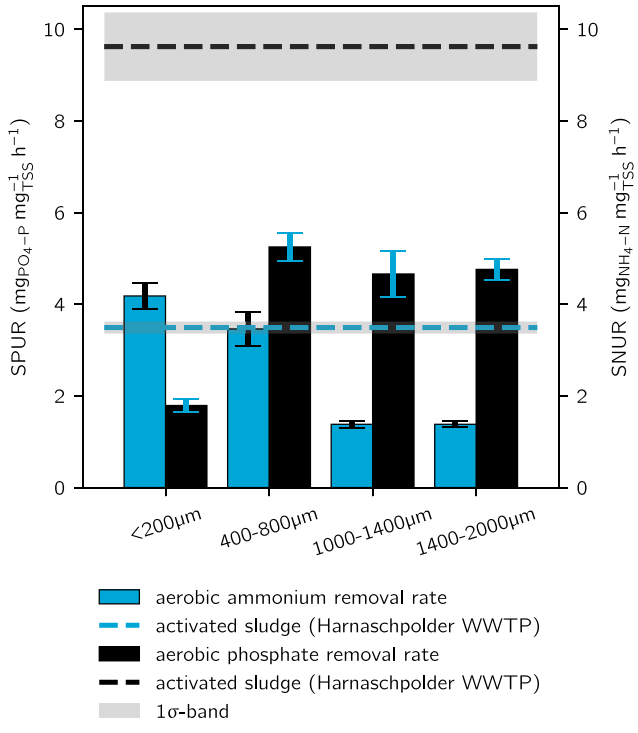

(a) Two alternating anaerobic upflow selectors (period I).

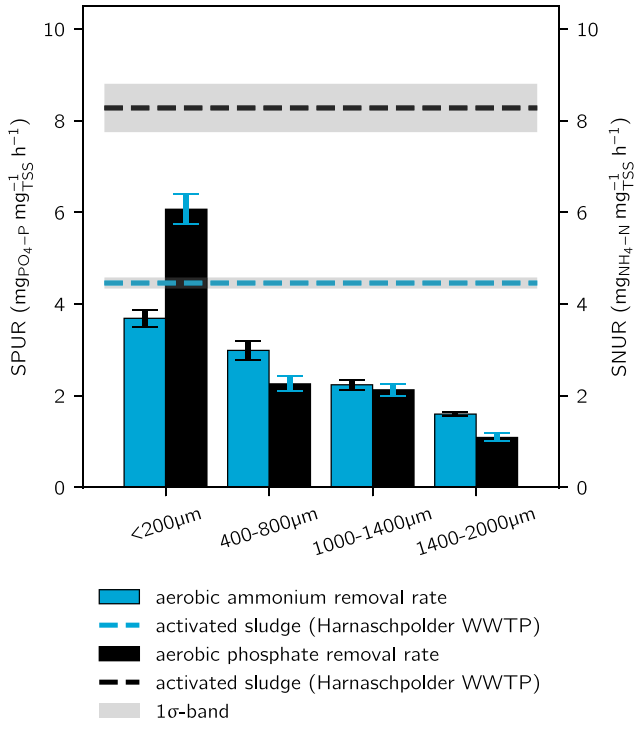

(b) Mixed anaerobic selector and anaerobic tank (period II).

Fig. 7. Maximum specific aerobic ammonium (SNUR) and phosphate removal (SPUR) rates for different sludge size fractions from the CFR pilot-scale CFR and the end of each operational period (bars) compared to the maximum specific rates determined for activated sludge from Harnaschpolder WWTP (dashed lines).

4. Discussion

This study investigated the potential growth of AGS in a CFAS system. The selective pressures responsible for aerobic granulation in a SBR, as proposed by van Dijk et al. (2022), were used to design a pilot-scale CFR. Metrics were defined for the extent to which mechanisms were implemented. The impact of the anaerobic distribution of GFS on granular growth were explicitly investigated. An anaerobic stage with bottom-feeding through an expanded sludge bed similar to a SBRs (period I) was compared to a configuration with a mixed anaerobic selector used in the CFAS system of the Harnaschpolder WWTP (period II).

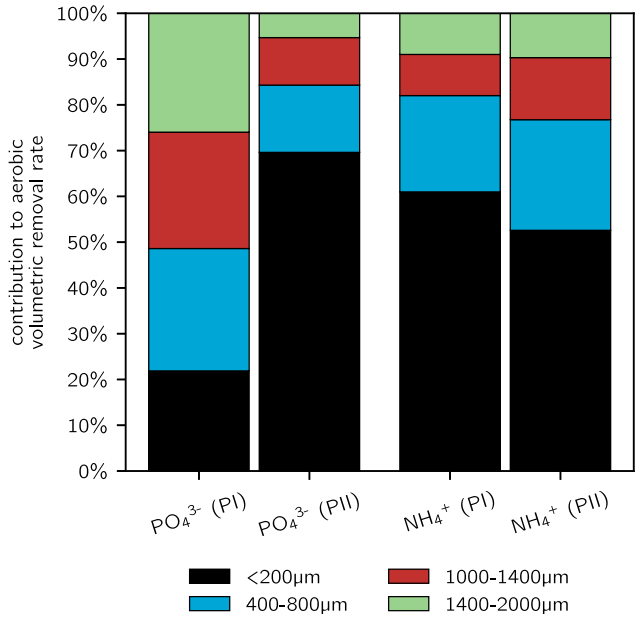

Fig. 8. Calculated contributions of each sludge size fraction to the total volumetric removal rates for ammonium and phosphate. The estimated maximum volumetric conversion rates for ammonium and phosphate for all size classes combined amounted to $-18.8\,mg_{PO_4-P}\,L^{-1}\,h^{-1}$ and $-15.7\,mg_{NH_4-N}\,L^{-1}\,h^{-1}$ for period I with the anaerobic upflow selectors, respectively, and to $-18.9\,mg_{PO_4-P}\,L^{-1}\,h^{-1}$ and $-15.2\,mg_{NH_4-N}\,L^{-1}\,h^{-1}$ for period II with the mixed anaerobic selector, respectively.

4.1. Implementation of mechanisms for growth of AGS from a SBR in a CFR

The first hypothesis was that sufficient growth of AGS could be achieved in a CFR treating pre-settled municipal wastewater, if the mechanisms for granulation proposed by van Dijk et al. (2022) were implemented to a similar extent as in a SBR. The biomass obtained using two alternating anaerobic upflow selectors showed similar properties to the seed sludge after 166 days of operation. The smoothness of the granular surfaces (Fig. 2) and the settleability were close to those reported for SBRs (Pronk et al., 2015; van Dijk et al., 2020). The MLSS concentration of the flocculent fraction (i.e. $2\,g_{TSS}\,L^{-1}$) was also similar. The maximum total MLSS concentration (i.e. $6.4\,g_{TSS}\,L^{-1}$) was lower than has been achieved in full-scale AGS-SBRs, where the large granule fraction >2 mm can yield total MLSS concentrations $>10\,g_{TSS}\,L^{-1}$ while maintaining the increased settleability compared to AS (Van der Roest et al., 2016; Pronk et al., 2015). Nevertheless, the selective enrichment of the granular sludge for EBPR activity using the anaerobic upflow selectors indicated that the AGS was obtained using the same selection principles as in full-scale AGS-SBRs.

4.1.1. Anaerobic distribution of granule forming substrate

Three aspects were studied determining the substrate distribution: microbial selection for anaerobic storage of GFS, maximizing transport of substrate into the granules and selective feeding. Complete conversion of the anaerobically storable fraction of $COD_{<0.45\ \mu m}$ was achieved (Table 3) and the degree of plug-flow in the expanded bed during the feeding phase (Fig. 4) was similar to full-scale SBRs (van Dijk et al., 2018). The extent of selective feeding of the largest granule size class was quantified by the retention probability in the expanded bed and the resulting average MLSS concentration in the bed of each size class (Fig. 5). There are no reports on this stratification in expanded beds of full-scale SBRs during feeding. However, the increasing retention probability for granules of increasing size was expected based on the ability of a Richardson-Zaki model to describe the settling of AGS (van Dijk et al., 2020), and the similar superficial velocity applied during feeding. The lower water depth of the upflow selector (2.5 m) did hamper the separation of flocs and granules due to limited volume above the granular bed, causing substantial parts of the granules >1000 µm and the 400–1000 µm to exit through the overflow (Fig. 5). Therefore, the height of the granular part of the expanded bed at the end of the feeding phase (1.05 m) was lower than in a full-scale AGS-SBR (1.4 m, van Dijk et al., 2020) with similar average MLSS and feeding velocity as used in this study (van Dijk et al., 2020). While the bed height was adequate for the complete removal of GFS, the stratification did not fully mimic that of full-scale AGS-SBRs, resulting in less selective feeding of the largest granules. The water depth of the anaerobic upflow selector is thus a critical design parameter for steering the GFS towards the largest granules.

Although all three mechanisms were implemented like in SBRs, these data are not sufficient to quantify that the anaerobic distribution of GFS was similar. A numerical modeling approach could be used in future work to integrate the information of all mechanisms to estimate the distribution of GFS, including the specific GFS conversion rates for individual size classes. Subsequently, the distribution could be compared to the distribution of GFS determined experimentally. The levels of intracellular storage polymers (i.e. PHAs and glycogen) would have to be determined for sludge from the expanded bed to construct a mass balance for GFS over the feeding phase (Haaksman et al., 2023). The distribution of granular growth could then be estimated for different anaerobic stage configurations in CFRs or SBRs (Kent et al., 2018; Devlin and Oleszkiewicz, 2018; Redmond et al., 2019), and to further test the assumptions of the framework by van Dijk et al. (2022).

4.1.2. Ratio of GFS to non-GFS

For the classification of GFS and non-GFS in the primary effluent of Harnaschpolder WWTP, a mapping was made from the characterization of different COD fractions as either GFS or non-GFS (Table 1). The fraction of $COD_{<0.45\ \mu m}$ was first equated to the available GFS because it was reported to closely match the maximum able to diffuse into full-scale AGS (van den Berg et al., 2022). Batch tests using activated sludge from Harnaschpolder WWTP were used to determine which part of the $COD_{<0.45\ \mu m}$ was anaerobically removed. Hydrolysis of particulate organic substrate and fermentation to soluble COD (Layer et al., 2019; van Dijk et al., 2022) to GFS were neglected using this method, and therefore the fraction of GFS might have been underestimated. Full-scale SBRs with AGS typically use raw wastewater as influent (Pronk et al., 2015; Toja Ortega et al., 2021; van Dijk et al., 2020), but implementation of AGS in CFAS systems will often rely on pre-settled wastewater (Wei et al., 2020). The impact of pre-settling on both process types should be studied further. Development of the methodology to determine the fraction of GFS is therefore needed. This is emphasized by the finding that initial specific biochemical oxygen demand (BOD) loading rate of mixed anaerobic selectors did not correlate with the observed degree of granulation (Wei et al., 2020). A standardized method has to be developed to determine the fraction of GFS in wastewater.

4.1.3. Redistribution of growth through erosion and breakage

Erosion and break-up of granules in the CFR was larger than in the AGS-SBRs at Utrecht WWTP (The Netherlands), since granule size class >2 mm was diminished several days after the initial seeding (see Fig. 3(a)). Erosion and breakage of the largest granular size class were sufficient to balance the growth in the pilot-scale CFR, while this balance is commonly reached at a larger maximum granule size in the referenced full-scale SBRs. The rate of detachment has been shown to increase per surface area increases for granular biofilms with increasing size due to the higher probability for particle collisions and the higher momentum of larger sludge particles (Gjaltema et al., 1997). Our findings are also consistent with work by de Graaff et al. (2020) showing that the rate of erosion for the same shear rate increases with granule size. Implementing AGS in CFRs requires transportation

of biomass between compartments, potentially yielding a larger energy input per volume than for SBRs. The typically lower water depth in aerated compartments of CFAS systems also requires a larger superficial gas velocity to achieve as similar volumetric oxygen transfer rates as in SBRs. Anoxic tanks in CFAS systems need mechanical mixing, contributing further to higher erosion rates of the granular sludge. The pilot-scale CFR required a specific energy input of 20 W m^{-3} for sludge suspension, which was higher than customary for full-scale CFAS systems (6 W m^{-3}, Bengtsson et al., 2019) and AGS-SBRs (3–12 W m^{-3}, van Dijk et al., 2018). The rate of detachment therefore decreases during scale-up to full-scale and will likely yield a larger maximum granule size.

4.1.4. Selective wasting of surplus sludge

Selective wasting was implemented in the CFR in a similar fashion as in SBRs (van Dijk et al., 2022) and yielded the expected increase in retention probability with increasing granule size (Fig. 6(a)). The probability for a sludge particle to be subjected to the selective wasting was different than in full-scale SBRs due to the intermittent discharge every 2.5 h. A sludge particle needed to be above the discharge manifold at the start of a discharge cycle like in full-scale AGS-SBRs, but also in a specific compartment. Still,a similar SVI_5/SVI_{30} ratio was obtained as has been reported for full-scale SBRs with the same MLSS concentration (Pronk et al., 2015) and was stable over time. This indicated that selective wasting was imposed to a similar extent. Selective wasting was done via removal of the top of a sludge bed after a settling phase. Sludge particles were therefore not separated based on the difference in terminal settling velocity, but rather on the ability to settle sufficiently fast given the properties of the sludge matrix. Selective sludge wasting based on settleability thus ensures increased retainment of better settling individual sludge particles, while at the same time providing control over the settleability of the sludge as a whole (van Dijk et al., 2020). This is different from other methods used to, for example, select for better settling densified AS using hydrocyclones (Avila et al., 2021; Ford et al., 2016; Roche et al., 2022; Gemza et al., 2022). These methods selectively waste and retain sludge based on properties affecting the settleability, but not the settleability itself.

4.2. Differences between selective pressures in SBRs and CFRs

4.2.1. Distribution of the ratio of anaerobic to aerobic/anoxic time

A similar degree of selective feeding was achieved with shallow anaerobic upflow selectors with a water depth of 2.5 m compared to full-scale AGS-SBRs of 7–7.5 m deep (Pronk et al., 2015; van Dijk et al., 2018). This design did cause part of the sludge to be washed out of the upflow selectors during the sludge accumulation phase and subsequent feeding phase. All size classes had a chance to be washed out, but the probability decreased with increasing granule size (Fig. 5). Flocculent sludge had a relatively longer residence time in the anoxic and aerobic stages, while granules >1 mm experienced the opposite. This might have contributed further to the enrichment of the flocs and small granules for more nitrification, while the EBPR activity was more present in the larger granules (Fig. 7(a)).

4.2.2. Residence time distribution of mixed anoxic and aerobic stages

The CFR design focused on translating the mechanisms for aerobic granulation from a SBR. Implicitly, it was assumed that the series of mixed anoxic and aerobic compartments behaved similar to the mixed phases in an SBR separated in time. The mixed tanks connected in series and the recycle flow from the aerobic stage to the anoxic stage of the CFR, however, exhibited the hydraulic RTD of an axial dispersion reactor with a large variance around the mean residence time. In AGS-SBRs all sludge is subjected to the selective pressures in synchronicity. The efficiencies of diverting substrate to the largest granules and selective discharge of excess sludge must be higher in a CFR than in a SBR to achieve the same stable granular sludge formation. This possibly contributed to the lower granular growth that was achieved. Existing CFAS systems often employ larger recycles than used in the pilot-scale CFR (van Nieuwenhuijzen et al., 2008), increasing the adverse effects.

4.3. Distribution of growth and activity depending on the anaerobic stage

The most apparent outcome was the stability of the granule size distribution in the CFR in both research periods, with and without selective feeding. The anaerobic upflow selectors used in period I were able to direct the available GFS towards the granular sludge fraction, which was reflected by the enrichment of all size classes >400 μm for a higher SPUR compared to the flocculent fraction (Fig. 7(a)). Therefore, the contribution of the granular size classes to the volumetric phosphate removal rate was 78%. As for the completely mixed anaerobic selector, all sludge fractions get equal access to substrate and the distribution is determined by the specific area of a size class. The specific area increases as the size of a sludge particle decreases, and therefore flocculent sludge and small granules are favored over larger granular size classes. In an anaerobic upflow selector, the larger granules can preferentially use the substrate due to the increased retention in the expanded bed. The disadvantage in specific area turns into an advantage in particle volume. We hypothesized that reducing the size advantage for granules using a completely mixed anaerobic compartment (period II) would lead to a decrease in the granular sludge fraction and the average granule size (van Dijk et al., 2022). Most notably, the change in anaerobic substrate distribution was manifested in the shift of the SPUR distribution from larger to smaller granules and flocs (Fig. 7(b)). The shift occurred within a several SRTs, indicating substantially less GFS was steered towards the granular size classes. Only a small decrease was observed in the mass distribution of the granules from the size class 1000–2000 μm to 400–1000 μm from period I to period II (Fig. 3). A lab-scale study using two anaerobic feeding methods yielded similar results (Haaksman et al., 2023) and it was hypothesized that the anaerobic distribution of GFS would be more critical when treating real sewage due to a lower rbCOD fraction in real wastewater (Rocktäschel et al., 2013; Layer et al., 2019). However in this study, the stability of the granular sludge morphology proved to be relatively large despite the limited growth. The selective retention of the granular sludge fraction was likely a strong contributor to maintaining the degree of granulation and exemplifies the compounding effect of multiple mechanisms (van Dijk et al., 2022). Although the completely mixed anaerobic feeding was sufficient to maintain good morphology and settleability, it is the authors' opinion that differences in EBPR activity indicated a higher stability of the AGS when anaerobic selective feeding via bottom-feeding was applied.

The distribution of the aerobic ammonium removal activity was also affected by the change in the anaerobic distribution of GFS, but to a smaller extent. The trend in the SNUR for period I decreased with increasing granule size, with a relatively large step from the size class 400–800 μm to 1000–1400 μm (Fig. 7(a)). The trend found in period II decreased more gradually with increasing granule size, and is congruent with the results from Nguyen Quoc et al. (2021) using a SBR with a mixed pulse-fed anaerobic phase. This configuration resembles the completely mixed anaerobic stage used in period II. The results from the current study support their hypothesis that the anaerobic bottom-feeding in full-scale AGS-SBRs would alter the distribution of nutrient removal activity compared to completely mixed pulse-feeding. However, we do believe that the current study has shown that bottom-feeding can also be employed in a CFR and that the anaerobic stage configuration is not restricted solely to completely mixed compartments. The anaerobic stage provides a way to control the distribution of the nutrient removal through the anaerobic distribution of GFS. Numerical models aiming to describe nutrient removal using AGS could be improved to capture these dynamics (Layer et al., 2020; Strubbe et al., 2022).

4.4. Treatment capacity in a CFR using AGS compared to a CFAS system

4.4.1. Biological treatment capacity

More than twofold higher volumetric removal rates were achieved for both phosphorus and nitrogen with the AGS in the pilot-scale CFR compared to the full-scale CFAS system of Harnaschpolder WWTP, treating the same pre-settled wastewater. This shows great potential for upgrading existing CFAS systems for higher loading rates and increased effluent quality. Multiple factors contributed to the larger biological treatment capacity. The degree of plug-flow of the anoxic and aerobic compartments of the pilot-scale CFR was substantially larger than the full-scale CFAS system due to the smaller recirculation factor of mixed liquor in the pilot-scale CFR (i.e. 2) compared to the full-scale CFAS system (i.e. 27, see supplementary materials). This means that for the CFAS system, there is a small concentration gradient in the mixed liquor from the beginning to the end of the combined aerobic and anoxic zones and concentrations are close to the final effluent concentrations. These concentrations are rate limiting and therefore volumetric removal rates are lower than in more compartmentalized reactors (Henze, 2007; Strubbe et al., 2022). For this reason the volumetric rates achieved in the full-scale reactor were lower than for the pilot-scale CFR, even though the SNURs and SPURs were larger for the AS compared to the AGS from the pilot-scale CFR (Fig. 7(a)). The higher MLSS concentration in the pilot-scale CFR further contributed to the larger volumetric treatment capacity. The full-scale CFAS system had a superior nitrogen removal due to limited optimization of the pilot-scale CFR for denitrification (Section 3.4.1), but the primary focus of this study was on the growth of AGS in a CFR and not on nutrient removal.

4.4.2. Hydraulic treatment capacity

The larger biological treatment capacity of the CFR with AGS was accompanied by a twofold increase in the sludge settleability compared to the CFAS system (i.e. $50\,mL\,g_{TSS}^{-1}$ versus $100\,mL\,g_{TSS}^{-1}$, respectively). A typical sludge volume loading rate for circular secondary clarifiers is $400\,L\,m^{-2}\,h^{-1}$ (Krijgsman, 2002). In comparison, full-scale AGS-SBRs are operated at an equivalent sludge volume loading rate in excess of $1000\,L\,m^{-2}\,h^{-1}$ during simultaneous feeding and effluent discharge (Pronk et al., 2015). Secondary clarifiers can therefore likely be operated at higher surface loading rates when using AGS, although the behavior of a mixture of flocculent and granular sludge requires further investigation in combination with the more complex hydrodynamics. The results of this study indicate that further optimization of the CFR concept can deliver a retrofit technology to increase capacity of CFAS systems.

5. Conclusions

Selective pressures responsible for aerobic granulation in full-scale AGS-SBRs were implemented in a pilot-scale CFR, fed with pre-settled municipal wastewater. The research focused on the role of the anaerobic distribution of GFS. The pilot-scale CFR can be developed further for process intensification in existing CFAS systems using AGS. Key findings of the study include:

- The selective pressures for growth of AGS applied in full-scale SBRs can be successfully translated to a CFR, fed with pre-settled influent from a municipal WWTP.
- Microbial selection for anaerobic removal of substrate and similar degrees of both of plug-flow and selective feeding of granular sludge can be combined in two continuously fed, alternating anaerobic upflow selectors, like AGS-SBRs.
- A more than twofold increase in the volumetric biological removal capacities for both phosphorus and nitrogen can be achieved compared to the full-scale CFAS system.
- Switching to a completely mixed anaerobic selector shifted the enhanced biological phosphorus removal activity from the granular sludge fractions to the flocculent sludge, while nitrification was mainly unaffected. This indicates a shift in anaerobic substrate distribution favoring the larger specific surface area of flocculent sludge, which is less favorable for the long-term stability of AGS, particularly with less acidified wastewater.

CRediT authorship contribution statement

Viktor A. Haaksman: Conceptualization, Data curation, Investigation, Methodology, Visualization, Writing – original draft, Writing – review & editing. **Edward J.H. van Dijk:** Conceptualization, Investigation, Methodology, Writing – original draft, Writing – review & editing. **Salah Al-Zuhairy:** Data curation, Investigation, Methodology, Validation. **Michel Mulders:** Conceptualization, Investigation, Methodology. **Mark C.M. van Loosdrecht:** Conceptualization, Funding acquisition, Methodology, Supervision, Writing – original draft, Writing – review & editing. **Mario Pronk:** Conceptualization, Methodology, Supervision, Writing – original draft, Writing – review & editing, Funding acquisition.

Declaration of competing interest

The authors declare the following financial interests/personal relationships which may be considered as potential competing interests: Viktor A. Haaksman, Mario Pronk and Edward J.H. van Dijk have patent #2027088 issued to HaskoningDHV Nederland BV. If there are other authors, they declare that they have no known competing financial interests or personal relationships that could have appeared to influence the work reported in this paper.

Data availability

The data that has been used is confidential.

Acknowledgments

The authors would like to express their gratitude to Rogier van Kempen for his aid in shaping the research plan, discussing outcomes and his unwavering dedication throughout the research. The support and hospitality of the staff at the Harnaschpolder WWTP were instrumental to project. We would like to thank Roel van de Wijgaart for his effort during the validation of the pilot-scale CFR. The contributions of Dion Boekelaar, Xiaoyan Lin, Daan van der Vorm and Wladimir Rios during the initial commissioning of the CFR are much appreciated. This work was supported by the Delfland Water Authority, Delfluent Services, Evides Industriewater, the Rijnland District Water Control Board and Royal HaskoningDHV.

Appendix A. Calculation procedures

A.1. Retention efficiency of anaerobic upflow selectors

The upflow selectors used as anaerobic stage imposed distribution in anaerobic retention time for sludge size classes depending on their settleability. Size classes unable to meet the selection criterion would overflow at the top during either the sludge accumulation phase or the feeding phase. The probability to be retained (P_{AN}) for each size class (i) was calculated based on sieve tests on sludge samples from both the return sludge and the expanded sludge bed at the end of the anaerobic feeding phase via Eq. (A.1). The expanded bed volume (V_{bed})

was determined via measurement of the bed height using a sludge blanket detector (SoliTechw^2 IR 0-10,000, Partech. St. Austell, UK).

$$P_{i,AN} = \frac{V_{bed} c_{i,bed}}{c_{i,MLSS} \frac{1+RSR}{RSR} F_{\text{influent}} t_{AN,s}} \quad (A.1)$$

The anaerobic retention probability per size class was used to calculate the anaerobic residence time ($RT_{i,AN}$) of a size class in an upflow selectors and the remaining RT in the aerobic/anoxic volume of the pilot-scale CFR (Eq. (A.2)). The distribution of each size class was compared to the hypothetical distribution based on the relative volume fractions of the anaerobic stage and the aerobic/anoxic stage, as if the sludge was completely mixed in all compartments.

$$RT_{i,AN} = \frac{2 \times V_{bed} c_{i,bed}}{2 \times V_{bed} c_{i,bed} + c_{i,MLSS} V_{AE/AO}} \quad (A.2)$$

A.2. Retention efficiency of selective sludge wasting

The efficiency of the selective sludge wasting based on settleability for each size class was calculated based on mixed samples taken from the compartment prior to the discharge of excess sludge, and from samples taken from the collected excess sludge. The probability to be retained (P_{WS}) was expressed as the fraction of the load of a size class (i) wasted using selective wasting, relative to the hypothetical load of a size class wasted without allowing the sludge to settle prior to the discharge (see Eq. (A.3)).

$$P_{i,WS} = 1 - \frac{c_{i,WS} V_{WS}}{c_{i,MLSS} V_{manifold}} \quad (A.3)$$

The SRT per size class (Eq. (A.4)) was calculated based on the measured selective sludge discharge load ($M_{i,WS}$), the number of discharge events per day (n_d), the amount of the sludge mass in the entire system of each size class ($M_{i,MLSS}$) and was related to the mean SRT ($\overline{SRT}$) for the total volume of the pilot-scale reactor (Eq. (A.5)).

$$SRT_i = \frac{M_{i,MLSS}}{n_d M_{i,WS}} \quad (A.4)$$

$$\overline{SRT} = \frac{\sum_i^N M_{i,MLSS}}{n_d \sum_i^N M_{i,WS}} \quad (A.5)$$

A.3. Hydraulic residence time distribution (RTD)

The mixing characteristics of the anaerobic stages used in both research periods were analyzed via determination of the residence time distribution. The concentration of ammonium in the influent of the pilot-scale CFR was used as a step-tracer ($c_{NH4-N,inf}$). First, the liquid in the compartment under study was completely displaced with effluent. The anaerobic compartment was then fed with influent as during normal operation for the same duration (t_{RTD}) and the concentration of ammonium in the outflow ($c_{NH4-N,out}$) was determined via grab samples at regular intervals. The cumulative RTD (F) and RTD (E) were computed based on the normalized tracer concentration via Eq. (A.6):

$$F(t) = \frac{c_{NH4-N,out}(t) - c_{NH4-N,eff}}{c_{NH4-N,inf}}, E(t) = \frac{dF(t)}{dt} \quad (A.6)$$

The mean residence time (first moment) and the normalized variance (second moment) were calculated via Eqs. (A.7) and (A.8):

$$t_m = \int_0^{t_{RTD}} tE(t)dt \quad (A.7)$$

$$\sigma^2 = \int_0^{t_{RTD}} (t - t_m)^2 E(t)dt \quad (A.8)$$

Appendix B. Supplementary data

Supplementary material related to this article can be found online at https://doi.org/10.1016/j.watres.2024.121531.

References

Avila, I., Freedman, D., Johnston, J., Wisdom, B., McQuarrie, J., 2021. Inducing granulation within a full-scale activated sludge system to improve settling. Water Sci. Technol. 84, 302–313. http://dx.doi.org/10.2166/wst.2021.006.

Beeftink, H.H., van den Heuvel, J.C., 1990. Bacterial aggregates of various and varying size and density: a structured model for biomass retention. Chem. Eng. J. 44, B1–B13. http://dx.doi.org/10.1016/0300-9467(90)80055-H, URL: https://www.sciencedirect.com/science/article/pii/030094679080055H.

Bengtsson, S., de Blois, M., Wilén, B.M., Gustavsson, D., 2019. A comparison of aerobic granular sludge with conventional and compact biological treatment technologies. Environ. Technol. 40, 2769–2778. http://dx.doi.org/10.1080/09593330.2018.1452985, publisher: Taylor & Francis. _eprint: http://dx.doi.org/10.1080/09593330.2018.1452985.

Daigger, G.T., Kuo, J., Derlon, N., Houweling, D., Jimenez, J.A., Johnson, B.R., McQuarrie, J.P., Murthy, S., Regmi, P., Roche, C., Sturm, B., Wett, B., Winkler, M., Boltz, J.P., 2023. Biological and physical selectors for mobile biofilms, aerobic granules, and densified-biological flocs in continuously flowing wastewater treatment processes: A state-of-the-art review. Water Res. 242, 120245. http://dx.doi.org/10.1016/j.watres.2023.120245, URL: https://www.sciencedirect.com/science/article/pii/S0043135423006814.

Daigger, G.T., Redmond, E., Downing, L., 2018. Enhanced settling in activated sludge: design and operation considerations. Water Sci. Technol. 78, 247–258. http://dx.doi.org/10.2166/wst.2018.287, URL:.

de Graaff, D.R., Dijk, E.J.H.v., Loosdrecht, M.C.M.v., Pronk, M., 2020. Strength characterization of full-scale aerobic granular sludge. Environ. Technol. 41, 1637–1647. http://dx.doi.org/10.1080/09593330.2018.1543357, publisher: Taylor & Francis _eprint: http://dx.doi.org/10.1080/09593330.2018.1543357.

De Kreuk, M.K., Van Loosdrecht, M.C.M.v., 2004. Selection of slow growing organisms as a means for improving aerobic granular sludge stability. Water Sci. Technol. 49, 9–17, URL: http://wst.iwaponline.com/content/49/11-12/9.

Delfluent Services, Evides Industriewater and the Delfland Water Authority, 2022. Delft blue Innovations research facility. URL: https://www.delftblueinnovations.nl/.

Devlin, T.R., Oleszkiewicz, J.A., 2018. Cultivation of aerobic granular sludge in continuous flow under various selective pressure. Bioresour. Technol. http://dx.doi.org/10.1016/j.biortech.2018.01.056, URL: http://www.sciencedirect.com/science/article/pii/S0960852418300695.

Figdore, B.A., David Stensel, H., Winkler, M.K.H., 2018. Bioaugmentation of sidestream nitrifying-denitrifying phosphorus-accumulating granules in a low-SRT activated sludge system at low temperature. Water Res. 135, 241–250. http://dx.doi.org/10.1016/j.watres.2018.02.035, URL: https://www.sciencedirect.com/science/article/pii/S0043135418301428.

Ford, A., Rutherford, B., Wett, B., Bott, C., 2016. Implementing hydrocyclones in mainstream process for enhancing biological phosphorus removal and increasing settleability through aerobic granulation. Proc. Water Environ. Fed. 2016, 2798–2811, URL: http://www.worldwaterworks.com/wp-content/uploads/2016/10/16A-Kennedy1.pdf.

Gemza, N., Janiak, K., Zięba, B., Przyszlak, J., Kuśnierz, M., 2022. Long-term effects of hydrocyclone operation on activated sludge morphology and full-scale secondary settling tank wet-weather operation in long sludge age WWTP. Sci. Total Environ. 845, 157224. http://dx.doi.org/10.1016/j.scitotenv.2022.157224, URL: https://www.sciencedirect.com/science/article/pii/S0048969722043224.

Giesen, A., de Bruin, L.M.M., Niermans, R.P., van der Roest, H.F., 2013. Advancements in the application of aerobic granular biomass technology for sustainable treatment of wastewater. Water Pract. Technol. 8, 47–54. http://dx.doi.org/10.2166/wpt.2013.007, URL: https://iwaponline.com/wpt/article/8/1/47/21384/Advancements-in-the-application-of-aerobic, publisher: IWA Publishing.

Gjaltema, A., Vinke, J.L., Loosdrecht, M.C.M.v., Heijnen, J.J., 1997. Abrasion of suspended biofilm pellets in airlift reactors: Importance of shape, structure, and particle concentrations. Biotechnol. Bioeng. 53, 88–99. http://dx.doi.org/10.1002/(SICI)1097-0290(19970105)53:1<88::AID-BIT12>3.0.CO;2-5, URL: https://onlinelibrary.wiley.com/doi/abs/10.1002/%28SICI%291097-0290%2819970105%2953%3A1%3C88%3A%3AAID-BIT12%3E3.0.CO%3B2-5, _eprint: https://onlinelibrary.wiley.com/doi/pdf/10.1002/%28SICI%291097-0290%2819970105%2953%3A1%3C88%3A%3AAID-BIT12%3E3.0.CO%3B2-5.

Haaksman, V.A., Schouteren, M., Loosdrecht, M.C.M.v., Pronk, M., 2023. Impact of the anaerobic feeding mode on substrate distribution in aerobic granular sludge. Water Res. 233, 119803. http://dx.doi.org/10.1016/j.watres.2023.119803, URL: https://www.sciencedirect.com/science/article/pii/S0043135423002385.

Henze, M. (Ed.), 2007. Activated Sludge Models ASM1, ASM2, ASM2d and ASM3, reprinted ed. In: Scientific and Technical Report / IWA, Number 9, IWA Publ, London, OCLC: 634487296.

Kent, T.R., Bott, C.B., Wang, Z.W., 2018. State of the art of aerobic granulation in continuous flow bioreactors. Biotechnol. Adv. 36, 1139–1166. http://dx.doi.org/10.1016/j.biotechadv.2018.03.015, URL: http://www.sciencedirect.com/science/article/pii/S0734975018300661.

Krijgsman, J., 2002. Optimalisatie van ronde nabezinktanks: Ontwerprichtlijnen en toepassing van het nabezinktankmodel : ontwerpen tussen STORA-1981 en solids flux theorie. In: STOWA;2002. Vol. 23, STOWA, Stichting Toegepast Onderzoek Waterbeheer [etc.], Utrecht [etc.], URL: https://edepot.wur.nl/118756.

Layer, M., Adler, A., Reynaert, E., Hernandez, A., Pagni, M., Morgenroth, E., Holliger, C., Derlon, N., 2019. Organic substrate diffusibility governs microbial community composition, nutrient removal performance and kinetics of granulation of aerobic granular sludge. Water Res. X 4, 100033. http://dx.doi.org/10.1016/j.wroa.2019.100033, URL: http://www.sciencedirect.com/science/article/pii/S2589914719300696.

Layer, M., Villodres, M.G., Hernandez, A., Reynaert, E., Morgenroth, E., Derlon, N., 2020. Limited simultaneous nitrification-denitrification (SND) in aerobic granular sludge systems treating municipal wastewater: Mechanisms and practical implications. Water Res. X 7, 100048. http://dx.doi.org/10.1016/j.wroa.2020.100048, URL: http://www.sciencedirect.com/science/article/pii/S2589914720300086.

Martins, A.M.P., Heijnen, J.J., van Loosdrecht, M.C.M., 2004a. Bulking sludge in biological nutrient removal systems. Biotechnol. Bioeng. 86, 125–135. http://dx.doi.org/10.1002/bit.20029, URL: http://onlinelibrary.wiley.com/doi/10.1002/bit.20029/abstract.

Martins, A.M.P., Pagilla, K., Heijnen, J.J., van Loosdrecht, M.C.M., 2004b. Filamentous bulking sludge—a critical review. Water Res. 38, 793–817. http://dx.doi.org/10.1016/j.watres.2003.11.005, URL: http://www.sciencedirect.com/science/article/pii/S004313540300616X.

Miyake, M., Hasebe, Y., Furusawa, K., Shiomi, H., Inoue, D., Ike, M., Enhancement of nutrient removal in an activated sludge process using aerobic granular sludge augmentation strategy with ammonium-based aeration control. Chemosphere 340, 139826. http://dx.doi.org/10.1016/j.chemosphere.2023.139826. URL: https://linkinghub.elsevier.com/retrieve/pii/S0045653523020957.

Nguyen Quoc, B., Wei, S., Armenta, M., Bucher, R., Sukapanpotharam, P., Stahl, D.A., Stensel, H.D., Winkler, M.K.H., 2021. Aerobic granular sludge: Impact of size distribution on nitrification capacity. Water Res. 188, 116445. http://dx.doi.org/10.1016/j.watres.2020.116445, URL: https://www.sciencedirect.com/science/article/pii/S0043135420309805.

Pronk, M., Abbas, B., Al-zuhairy, S.H.K., Kraan, R., Kleerebezem, R., Loosdrecht, M.C.M.v., Effect and behaviour of different substrates in relation to the formation of aerobic granular sludge. Appl. Microbiol. Biotechnol. 99, 5257–5268. http://dx.doi.org/10.1007/s00253-014-6358-3. URL: http://link.springer.com/article/10.1007/s00253-014-6358-3.

Pronk, M., de Kreuk, M.K., de Bruin, B., Kamminga, P., Kleerebezem, R., van Loosdrecht, M.C.M., 2015. Full scale performance of the aerobic granular sludge process for sewage treatment. Water Res. 84, 207–217. http://dx.doi.org/10.1016/j.watres.2015.07.011, URL: http://www.sciencedirect.com/science/article/pii/S0043135415301147.

Redmond, E., Jalbert, M., Young, M., Faraj, R., Sturm, B., Downing, L., 2019. Full-scale continuous flow selective pressures for sludge granulation. In: Proceedings, Water Environment Federation. pp. 3490–3497, URL: https://www.scopus.com/inward/record.uri?eid=2-s2.0-85075029645&partnerID=40&md5=3a0b05db678e012e4603e33d724fb266. type: Conference paper.

Roche, C., Donnaz, S., Murthy, S., Wett, B., 2022. Biological process architecture in continuous-flow activated sludge by gravimetry: Controlling densified biomass form and function in a hybrid granule-floc process at Dijon WRRF, France. Water Environ. Res. 94, e1664. http://dx.doi.org/10.1002/wer.1664.

Rocktäschel, T., Klarmann, C., Helmreich, B., Ochoa, J., Boisson, P., Sørensen, K.H., Horn, H., 2013. Comparison of two different anaerobic feeding strategies to establish a stable aerobic granulated sludge bed. Water Res. 47, 6423–6431. http://dx.doi.org/10.1016/j.watres.2013.08.014, URL: http://www.sciencedirect.com/science/article/pii/S0043135413006544.

Strubbe, L., Pennewaerde, M., Baeten, J.E., Volcke, E.I.P., 2022. Continuous aerobic granular sludge plants: Better settling versus diffusion limitation. Chem. Eng. J. 428, 131427. http://dx.doi.org/10.1016/j.cej.2021.131427, URL: https://www.sciencedirect.com/science/article/pii/S1385894721030084.

Toja Ortega, S., Pronk, M., de Kreuk, M.K., 2021. Effect of an increased particulate COD load on the aerobic granular sludge process: A full scale study. Processes 9 (1472), http://dx.doi.org/10.3390/pr9081472, URL: https://www.mdpi.com/2227-9717/9/8/1472. number: 8 Publisher: Multidisciplinary Digital Publishing Institute.

van den Berg, L., Toja Ortega, S., van Loosdrecht, M.C.M., de Kreuk, M.K., 2022. Diffusion of soluble organic substrates in aerobic granular sludge: Effect of molecular weight. Water Res. X 16, 100148. http://dx.doi.org/10.1016/j.wroa.2022.100148, URL: https://www.sciencedirect.com/science/article/pii/S2589914722000184.

Van der Roest, H., van Bentem, A., Uijterlinde, C., de Man, A., 2016. Nereda technology shows a steep growth curve. H2O/Water Matters 2, URL: https://www.h2o-watermatters.com/?ed=201612#.

van Dijk, E.J.H., Haaksman, V.A., van Loosdrecht, M.C.M., Pronk, M., 2022. On the mechanisms for aerobic granulation - model based evaluation. Water Res. 216, 118365. http://dx.doi.org/10.1016/j.watres.2022.118365, URL: https://www.sciencedirect.com/science/article/pii/S004313542200327X.

van Dijk, E.J.H., Pronk, M., van Loosdrecht, M.C.M., 2018. Controlling effluent suspended solids in the aerobic granular sludge process. Water Res. 147, 50–59. http://dx.doi.org/10.1016/j.watres.2018.09.052, URL: http://www.sciencedirect.com/science/article/pii/S004313541830767X.

van Dijk, E.J., Pronk, M., van Loosdrecht, M.C., 2020. A settling model for full-scale aerobic granular sludge. Water Res. 186, 116135. http://dx.doi.org/10.1016/j.watres.2020.116135, URL: https://linkinghub.elsevier.com/retrieve/pii/S0043135420306722.

Van Loosdrecht, M.C.M., Nielsen, P.H., Lopez-Vazquez, C.M., Brdjanovic, D. (Eds.), 2016. Experimental Methods in Wastewater Treatment. IWA Publishing, London.

van Nieuwenhuijzen, A.F., van Bentem, A.G.N., Buunnen, A., Reitsma, B.A., Uijterlinde, C.A., 2008. The limits and ultimate possibilities of technology of the activated sludge process. Water Sci. Technol. 58, 1671–1677. http://dx.doi.org/10.2166/wst.2008.545.

Wei, S.P., Stensel, H.D., Quoc, B.N., Stahl, D.A., Huang, X., Lee, P.H., Winkler, M.K.H., 2020. Flocs in disguise? High granule abundance found in continuous-flow activated sludge treatment plants. Water Res. 115865. http://dx.doi.org/10.1016/j.watres.2020.115865, URL: http://www.sciencedirect.com/science/article/pii/S0043135420304024.

Winkler, M.K.H., van Loosdrecht, M.C.M., 2022. Intensifying existing urban wastewater. Science 375, 377–378. http://dx.doi.org/10.1126/science.abm3900, URL: https://www-science-org.tudelft.idm.oclc.org/doi/10.1126/science.abm3900. publisher: American Association for the Advancement of Science.